1964

A study of the energy required to erode single crystal beta tin by the electro discharge machining process

Anthony E. Peter
Lehigh University

A STUDY OF THE ENERGY REQUIRED TO ERODE SINGLE CRYSTAL BETA TIN BY THE ELECTRO DISCHARGE MACHINING PROCESS

by

Anthony E. Peter

A THESIS

Presented to the Graduate Faculty

of Lehigh University

in Candidacy for the Degree of

Master of Science

Lehigh University

1964

This thesis is accepted and approved in partial fulfillment for the degree of Master of Science.

Date May 19, 1964

Professor in Charge

Head of the Department of
Metallurgical Engineering

Acknowledgments

The author wishes to thank the many members of the Western Electric Engineering Research Staff and in particular the following:

A. L. Hatcher and D. H. Pruden for their assistance on the electrical circuitry,

R. B. Palme for project supervision and the latitude for experimentation given me,

T. P. Turnbull for some of the electron microscopy work, and

Dr. J. D. Wood, Lehigh University, my advisor.

Table of Contents

Figures

Figures

Tables

Abstract

A method for measuring the relative total energy required to electro discharge machine materials was evolved by modification of the circuitry of a commercial electro discharge machine.

Single crystal beta tin was machined in two crystallographic orientations using a brass electrode to determine if the anisotropic properties of the tin would affect the total energy required in the machining process.

The expected energy difference due to anisotropy was masked by

1.) a polycrystalline layer of copper from the brass deposited on the tin,

2.) a polycrystalline layer of tin formed on the single crystal being machined,

3.) severe deformation in the single crystal subsurface, and

4.) the inability to control accurately or monitor the gap spacing and dielectric contamination.

The Electro-Discharge Machining Process

Since 1943 when B. R. and N. I. Lazarenko (1) proposed the use of a resistance-capacitance type generator circuit for the machining of metals, much interest and effort has been directed to the commercial use of the process.

The Electro-discharge machining process, hereinafter called EDM, basically consists of a generator or power supply circuit capable of applying a pulsed type wave form to two electrodes immersed in a liquid dielectric. When these electrodes are so positioned with respect to each other that the gap between them is on the order of .001 inch and the voltage between them is sufficient to overcome the gap-dielectric combination, a rather violent spark traverses the gap and material is removed from both electrodes. The spark is extinguished after the pulse is completed and occurs again on the next voltage pulse if the gap-dielectric conditions for spark initiation are met. This might be accomplished by repositioning the electrodes if much erosion has occurred or by increasing the potential between them.

Many types of commercial EDM machines have been marketed in the past twenty years. They are in essence, a quill or tool holder driven by a servo mechanism which senses the gap condition (shorted or open circuit) and a generator. Refinements such as variable voltage, capacitance and current, variable feed rate, vibration of the tool, dielectric circulation and filtering have been added for better control of erosion rate and surface finish so necessary in commercial applications.

The major use of EDM machines is by the die sinking industry but important applications are being made to machine extremely unmachinable

conductive materials and to make shapes or holes difficult to produce by conventional methods.

The process is essentially a reproductive one. The tool, normally the negative electrode is fabricated from an easily machinable material such as brass, steel or carbon such that it is a negative image of the desired finished contour on the workpiece, the positive electrode. Except for tool wear, the impression on the workpiece after erosion is the desired shape.

The Mechanism of Metal Removal-- Current Theories

The literature abounds in speculation on the metal removal mechanism. The following theories are currently the most popular:

Melting Theory

First the material is locally melted by the high current densities passing through the gas column in the dielectric, then the particles are ejected from the melted zone by a pressure wave. (2) (3)

Field Effect Theory

The large current density pulses inherent in the process create extreme local voltage gradients in the surface of the material being eroded. These gradients are sufficient to overcome the tensile strength of the material and particles are torn off. (4) (5) (6)

Electron Avalanche Theory

An electron avalanche is started by emission from the cathode due to the potential. This emission is greatly intensified by ionization of the dielectric. The metal removal in this case is effected by impingement of this avalanche on the material being eroded. (7)

To a reader of the EDM literature it is confusing to find diametrically opposite viewpoints supported by graphs and data purporting to prove the writer's hypothesis for the material removal mechanism. For example, Williams (4) concludes definitely that material is removed without melting and shows that there is quantitative correlation between erosion and the field forces created by the localized voltage gradients. Toth-Bitskey (6) supports this thesis by concluding that erosion is not determined by the heating effects of the spark discharges but predominantly by field strength and electrodynamical forces.

On the other hand Barash (2) on the basis of high speed photography (500,000 frames/sec.) is convinced that the phenomenon consists of formation of a discharge column of low electrical resistance and extremely small diameter which is probably initiated by foreign matter in the dielectric. This is followed by the passage of current of high density due to the small column area, localized or surface melting and vaporization of the material being eroded, then expulsion of the molten material by the sound wave, created by the spark, and aided by the expansion of gases dissolved in the material. Opítz (3) concurs on the basis that in steels a martensitic layer is formed. Quenching is effected by the inrush of the cool dielectric when the discharge column collapses. Although this implies that a necessary condition would be temperatures above A_{C_3}, this does not constitute proof for melting. The ejected particles, according to Dr. Opitz, also suggest melting since they are spherical. It could be presumed that surface tension on the molten masses would be responsible for this least area/volume configuration prior to resolidification.

A Model for Material Removal

The above anomalies led the author to consider whether an experiment could be constructed to either reduce the number of theories, clarify the existing problem or to produce enough evidence for the formulation of the true mechanism of metal removal in the electro-discharge machining process.

It was felt that if the field effect theory has merit, an analysis of a model based on the rupturing of atom to atom bonds would at least indicate whether an experiment could have any possibility of positive results. Neglecting in what manner such a field might distribute itself within any given material, it is considered that particles of a single crystal lattice might be separated from a single crystal in the form of hemispheres. Consider a single crystal having the growth axis in the [001] direction, with four-fold symmetry about that axis, being machined along the $[00\bar{1}]$ direction. The projected area of the hemisphere in the [010] , $[0\bar{1}0]$, [100] , $[\bar{1}00]$ and $[00\bar{1}]$ directions divided by the respective areas of a unit cell in the same directions would, in the case of a simple cubic lattice, be representative of the number of nearest neighbor bonds broken. If it is hypothesized that

$$W \propto \frac{1}{b^n}$$

that is to say the energy or work is inversely proportional to the bond length, "b", to some power $n \geq 1$ then the sum of the broken bonds, assuming some particle size, could be determined and the energy required to remove a given amount of material from the crystal could be

found as a function of "n". The absolute energy could not be determined by this technique without a knowledge of the magnitudes of "n" and the proportionality constant required for the equality, however, if a crystal of less than the maximum symmetry were chosen, a ratio of the energy or work required to break bonds in one crystallographic direction to the energy required to break bonds another direction could be expressed as a function of "n" since the constant would presumably cancel out in the ratio.

Appendix I contains the mathematics used, considering nearest and next nearest neighbor bond rupture, and reiterates the assumptions made above. For beta-tin, a body centered tetragonal lattice, where W_{001} and W_{100} is the work required to remove a hemisphere of material, the results are as follows for the orientations subscripted:

n	W_{001}/W_{100} / 1.25
1	
2	1.52
3	1.70
4	1.77

Purpose and Objectives--EDM and Anisotropy

On the basis of the above calculations it was decided to:

1. Devise a method of measuring the energy required to EDM a material,
2. Machine a material in two orientations of extreme d spacing, measuring both energy and weight of material removed, and
3. Accept the hypothesis above if a specific energy difference (energy/unit weight) due to crystallographic orientation was

measured and determine the exponent "n".

Experimental Procedure

Machine Used

The Electro-discharge machine used in this study was a 1.5 kw Agietron manufactured by Agie Company, Locarno, Switzerland, Model AB 1.5 serial number 15.041, henceforth referred to as Agietron (Fig. 1). The oscilloscope and counter shown are accessory equipment required for the experiment.

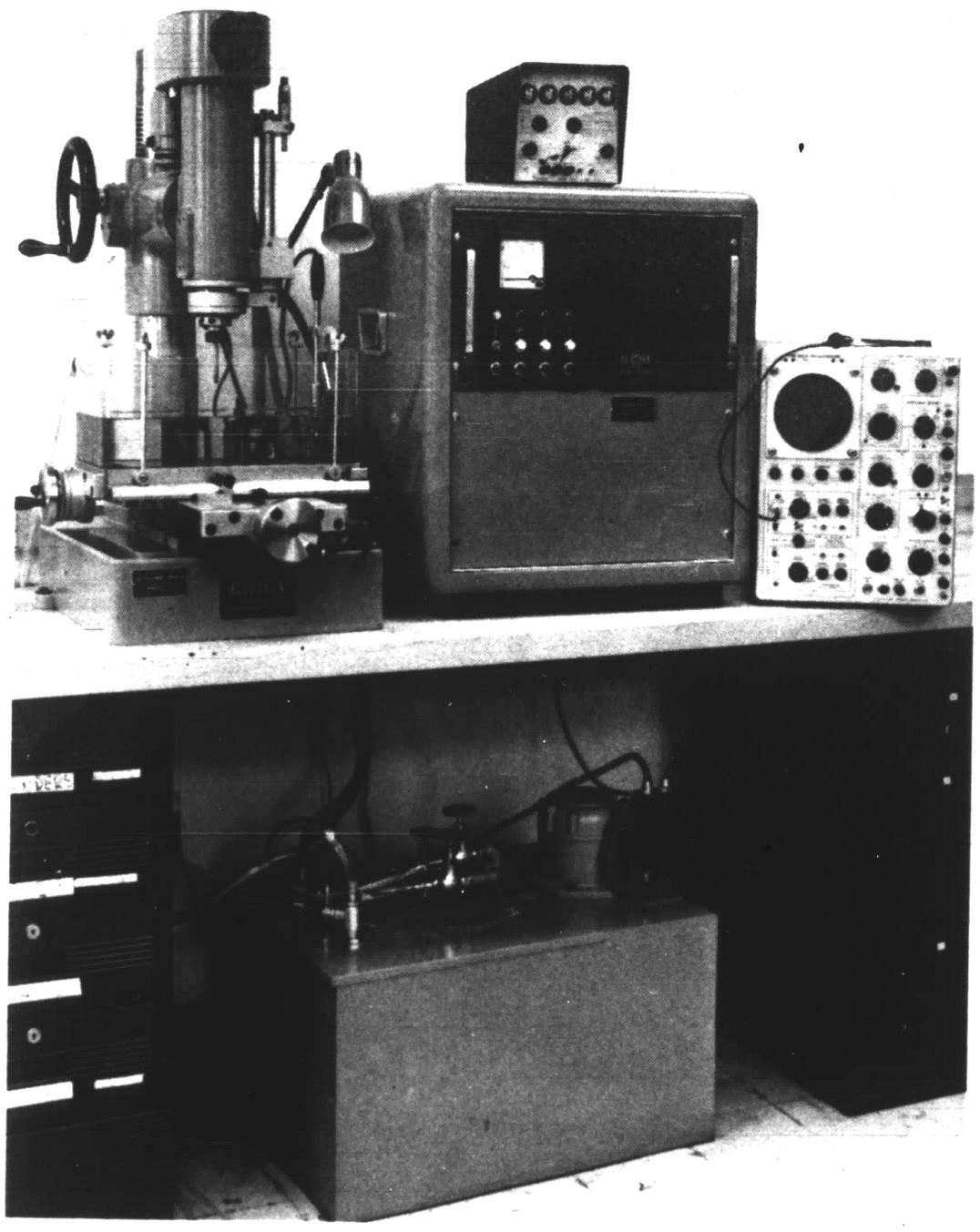

Figure 1 AB 1.5 Agietron EDM machine with oscilloscope and pulse counter installed

The above Agietron has an electro-mechanical 60 cycle vibrating tool holder to assist in removal of erosional debris from the machining gap. The vibration amplitude has variable control. The quill or work head can be advanced and retracted by a handwheel but a servomotor system which senses voltage across the gap is used while machining. This system detects whether there is a potential difference or a short between the tool (cathode) and workpiece (anode). If there is a voltage difference, the servomotor will drive the quill towards the workpiece at a preselected feed rate.

If a short is sensed, the motor will retract the quill until a gap and thus a voltage difference is once again established.

Additional machining parameter controls are step selection of 1 through 7 for voltage (V), current (J) and capacitance (C) values. A settling tank with two parallel one micron filters and a vane type, constant speed pump circulates the dielectric fluid to maintain a relatively low level of dielectric contamination. The dielectric flow is controlled by a manually operated valve. The pump capacity is overadequate and results in a dielectric temperature rise, the effects of which are discussed in a later section of this paper.

Ideal and Actual Voltage Waveforms

Since the machine is of the resistance-capacitance (R-C) type, shown schematically in Figure 2, there immediately arises problems in measurement of the total energy used in the erosion process. In the R-C circuit, the direct current or rectified alternating current power supply (PS) charges the capacitor (C) through the limiting

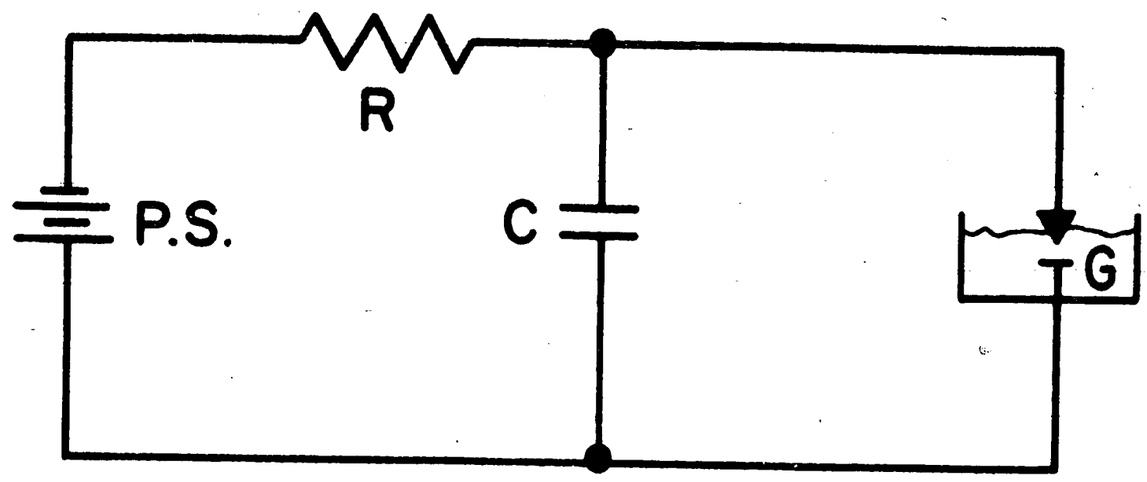

Figure 2 Simplified schematic of R-C EDM circuit

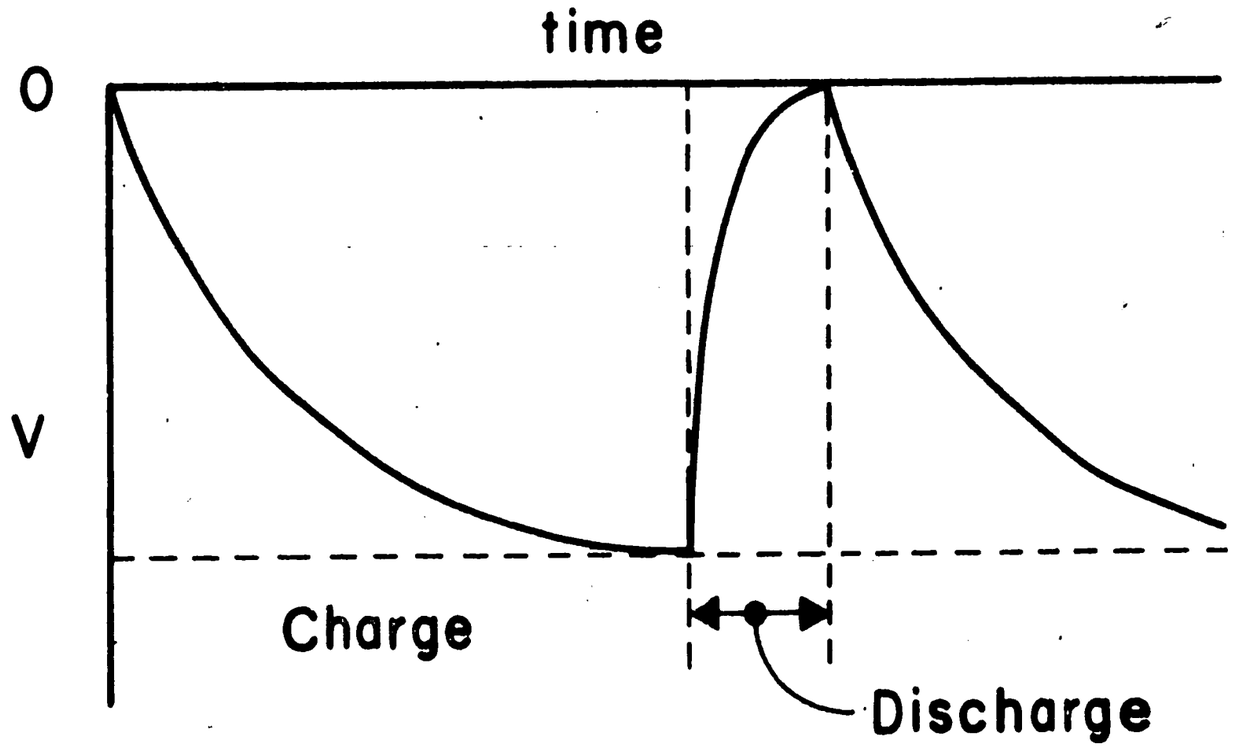

Figure 3 Idealized wave form of R-C circuit in EDM operation

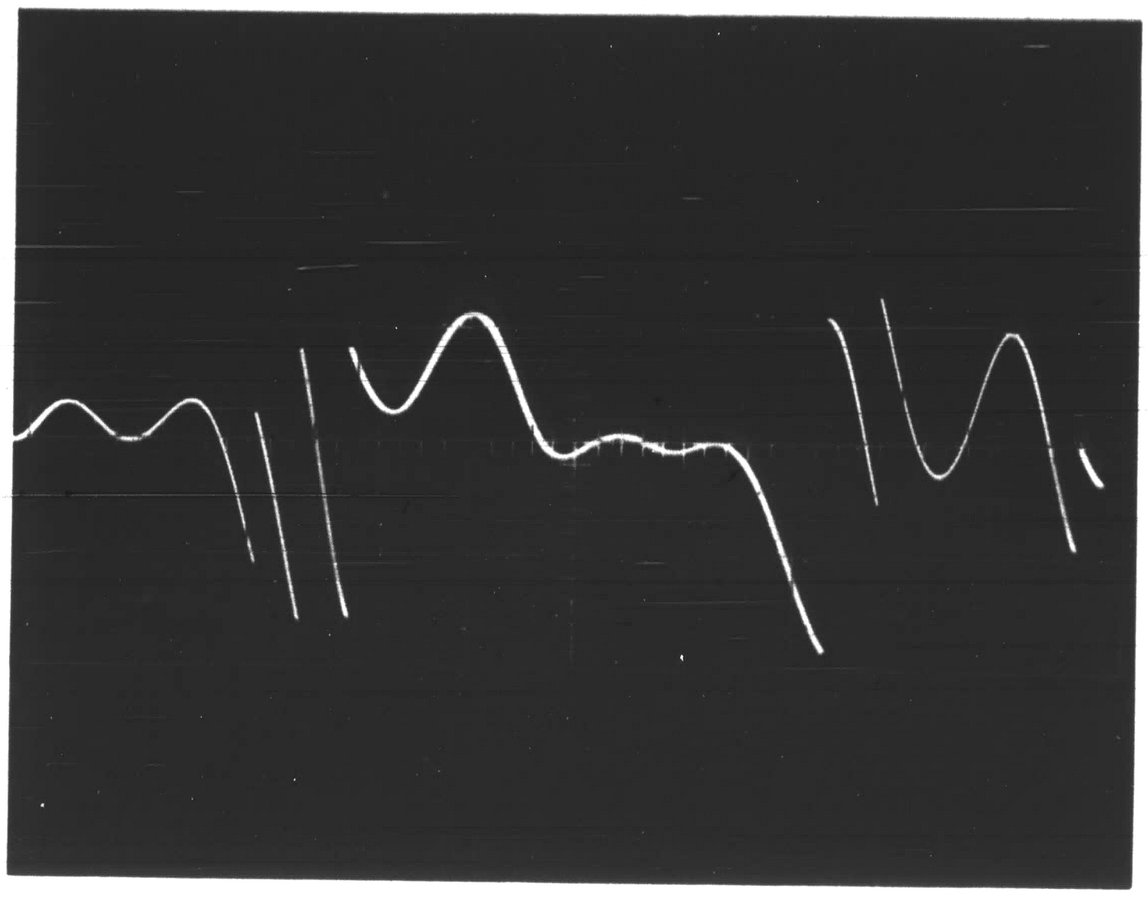

Figure 4 Voltage wave form of Agietron machine as purchased - machining mode operation. Vertical base 50v/cm, time base 20 ms/cm.

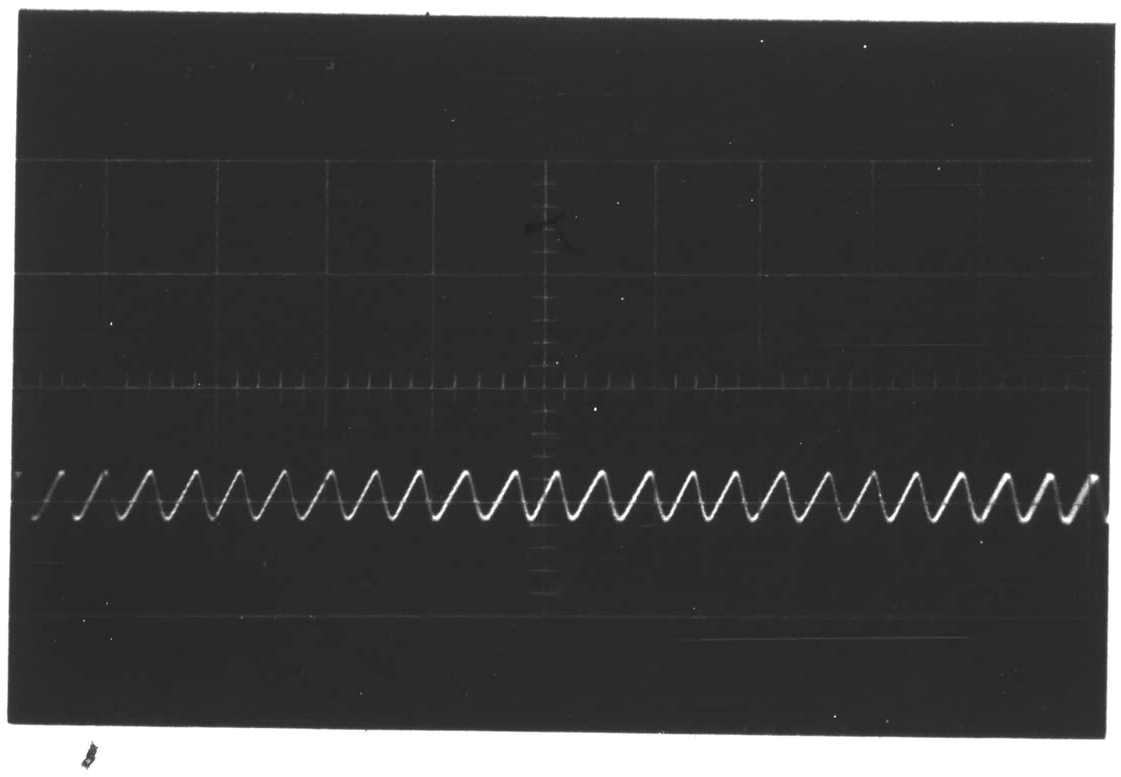

Figure 5 Peak-to-peak voltage wave form of Agietron power supply. Vertical base 50v/cm, time base 20 ms/cm.

resistance (R). Varying R and/or C varies the frequency at which the circuit can charge and discharge through the gap (G), provided the gap is held at constant separation under the dielectric. Ideally the voltage wave form in such a circuit would appear as in Figure 3.

The voltage wave form of the Agietron machine as purchased was recorded by oscilloscope and is shown on Figure 4.

From Figure 4 it can be seen that the discharges are occurring at random voltages. The ripple noticeable during the charging cycle is due to imperfections in the design of the power supply. Figure 5 shows the power supply ripple when the machine is in operation but in a non-discharging mode. Peak to Peak variation is 135V to 160V.

Methods of Measuring Energy Expended at the Gap

As material is being eroded from the workpiece, some amount of energy is being used. Several methods of measuring the specific amount of energy are feasible. Since the relationship,

$$J = EIt$$

where J = energy in each pulse

E = voltage

I = current

t = time

is a definition of energy and since the current and voltage are varying randomly both in amplitude and duration, it appeared that one of

the following methods might be feasible for the energy determination:

Method 1. Read the energy used directly from a device, such as a watt hour meter, or

Method 2. Record the voltage and current wave forms of each pulse, as a function of time, determine the product E x I versus time for each pulse, integrate this product versus time and sum for all pulses while a measurable amount of material was removed, or

Method 3. Assume that, for instance, in a million pulses there is some average pulse. Determine the current and voltage wave form of this average pulse versus time, integrate the product E x I over the time for the average pulse and multiply by the number of pulses observed during the time an amount of material was removed, or

Method 4. Modify the machine circuitry such that the capacitor bank must always charge up to a set voltage before allowing a discharge to occur. Since the energy (E) stored in a capacitor (C) charged to a voltage (V) is

$$E = \tfrac{1}{2}CV^2$$

and since the capacitor completely discharges during a pulse, it would then be necessary only to determine the energy of

a pulse and multiply by the number of pulses.

Circuit Development

Since reading the energy directly appeared to be the simplest approach of the above four methods, a search of the literature for a suitable meter was made without success. In general, watt hour meters depend on the input being, if not sinusoidal, at least regular. A recent development, the Hall effect device, seemed to offer a possible solution. The Hall effect is a phenomenon such that if a magnetic field (B) is impressed at right angles to an electrical current (I) in a conductor, a voltage difference (V) appears at right angles to both field and current which is proportional to the product of field and current. (See Figure 6)

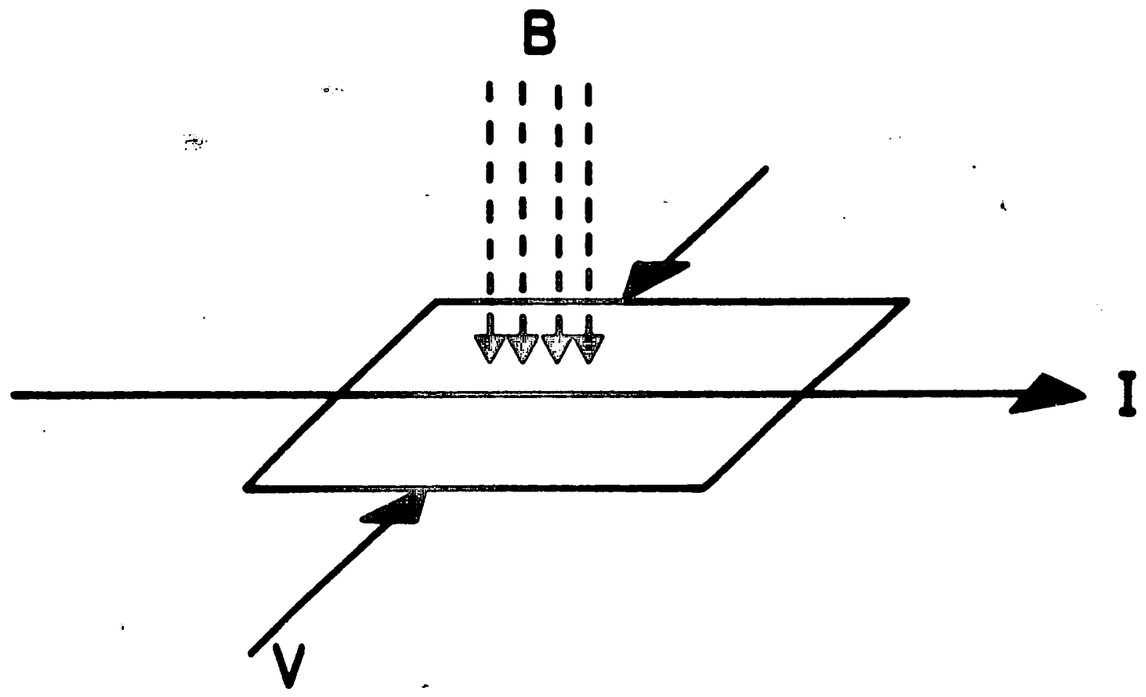

Figure 6 Simplified schematic of a Hall effect device

It was thought that if the magnetic field (B) could be made proportional to the current flowing through the gap by inserting one of

the leads leading to the gap through a slotted toroidal ferrite concentrator core and if current (I) was made proportional to the potential across the gap by bridging the gap with a relatively high resistance, which would have little effect on the gap, then the output of the Hall device inserted in the slotted coil would be proportional to the E I product. A d-c amplifier and integrating circuit was built to increase and sum the cell output. In operation, the Hall cell could not respond to the high frequencies in the gap and the integrator would saturate in a few minutes due to the unavoidable drift of the d-c amplifier.

Methods 2 and 3 were studied for feasibility but were considered impractical. Each would have necessitated cine-photography of oscilloscope traces and manual integration of current and voltage wave forms.

The feasibility of forcing the capacitors to charge to a fixed voltage before allowing any discharges to occur, as suggested in method 4, was studied. The need for a gating device with good response characteristics and the ability to pass large currents was of prime concern. A silicon controlled rectifier (SCR) was considered the only device meeting the above criteria and a circuit (Figures 7 and 8) was devised and built.

Consider negative as ground. As the positive voltage is increasing, the capacitor is charging. Zener Diode D1 was chosen such that its breakdown voltage was slightly below the voltage desired for the capacitor discharge. As the charging voltage exceeds the D1 voltage a small current will flow in the R - D1 leg and due to the current through R, a voltage will develop across R and point "a" will become

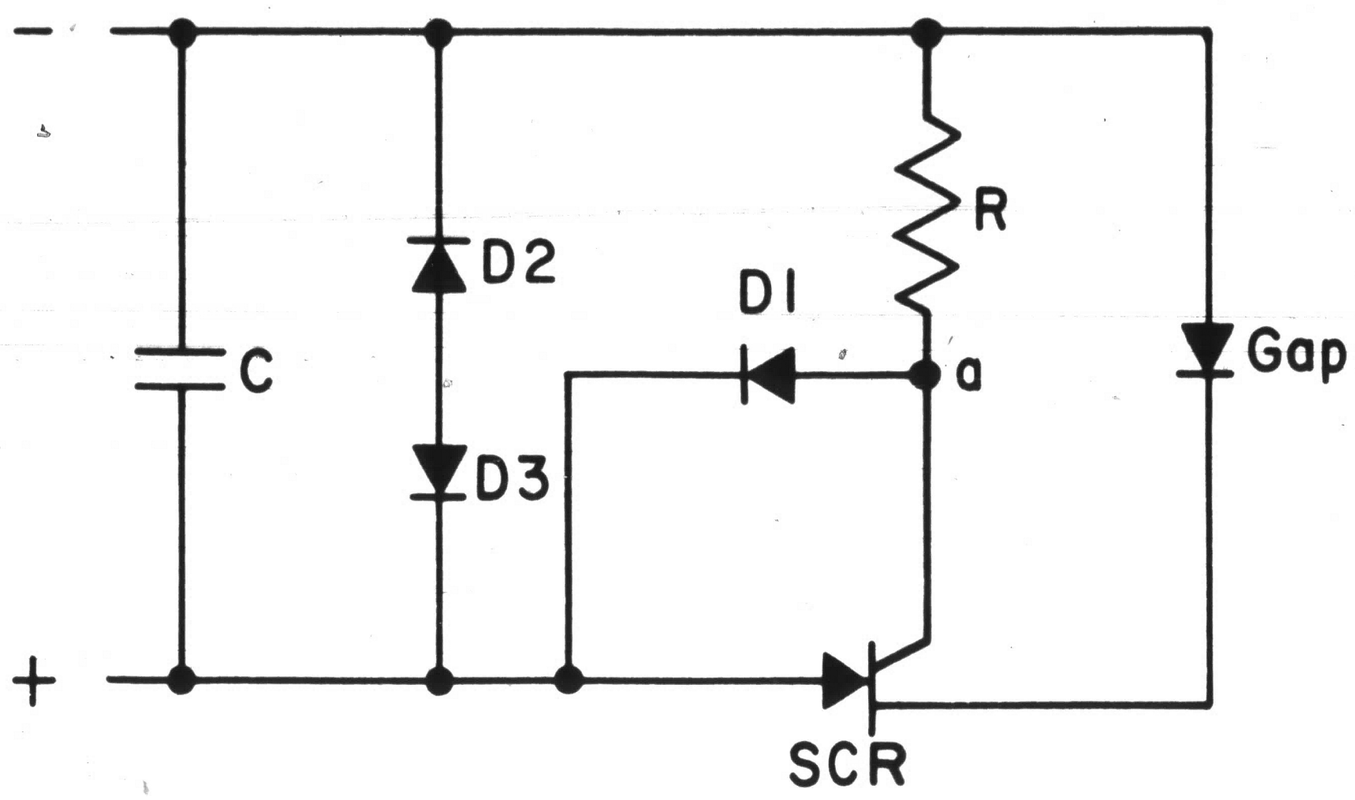

Figure 7 Schematic of SCR circuit

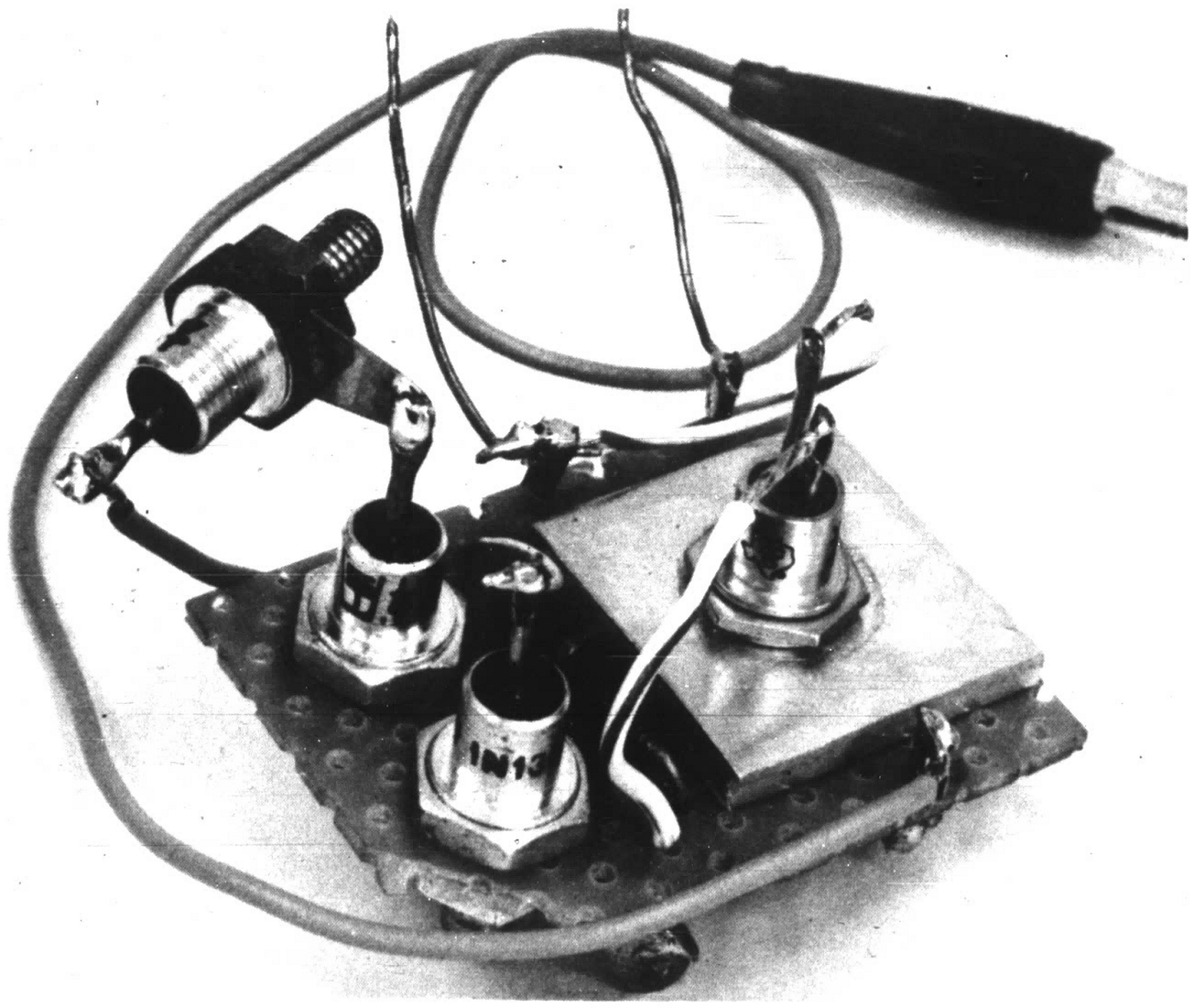

Figure 8 SCR circuit board

positive. As soon as point "a" is positive, the SCR will conduct or switch on and if the gap is such that the applied voltage will break down the dielectric, then a discharge will occur and erosion will follow. If the gap is too far open, the circuit will be an open circuit and nothing will occur. If the gap is non-existent or shorted, no erosion will take place. As soon as the discharge starts to occur, the voltage across the R - D1 leg drops, current ceases to flow in the leg and point "a" returns to ground potential. When the discharge is over, the SCR returns to non-conductivity until the necessary 150V appears across the leg once more. Due to the inevitable inductance in leads, components, etc., it was necessary to add Zener Diodes D2 and D3 to reduce ringing or reversed polarity pulses which caused electrode wear. On normal polarity, D3 is chosen higher than any expected pulse size, say 200V, so that it acts as an open circuit to the charging voltage. On a reversed polarity pulse D3 will conduct, but D2 is chosen to break down at very low voltages, say 5V, so that little or no reverse erosion will occur at the gap due to this voltage. This circuit was incorporated in the machine and the resultant wave form is shown in Figure 9.

It can be seen from the Figure 9 that the voltage at which the discharge is starting although just above 150V is varying probably due to variation in ripple voltage or gap conditions discussed later. A final modification was made by placing a selected string of Zener Diodes with 152V breakdown in D3 position to minimize the effect of the ripple voltage by conducting during the ripple peaks. This final modified circuit would now allow the capacitor to discharge only after it charged to above 150V and would not allow it to charge to over 152V. The

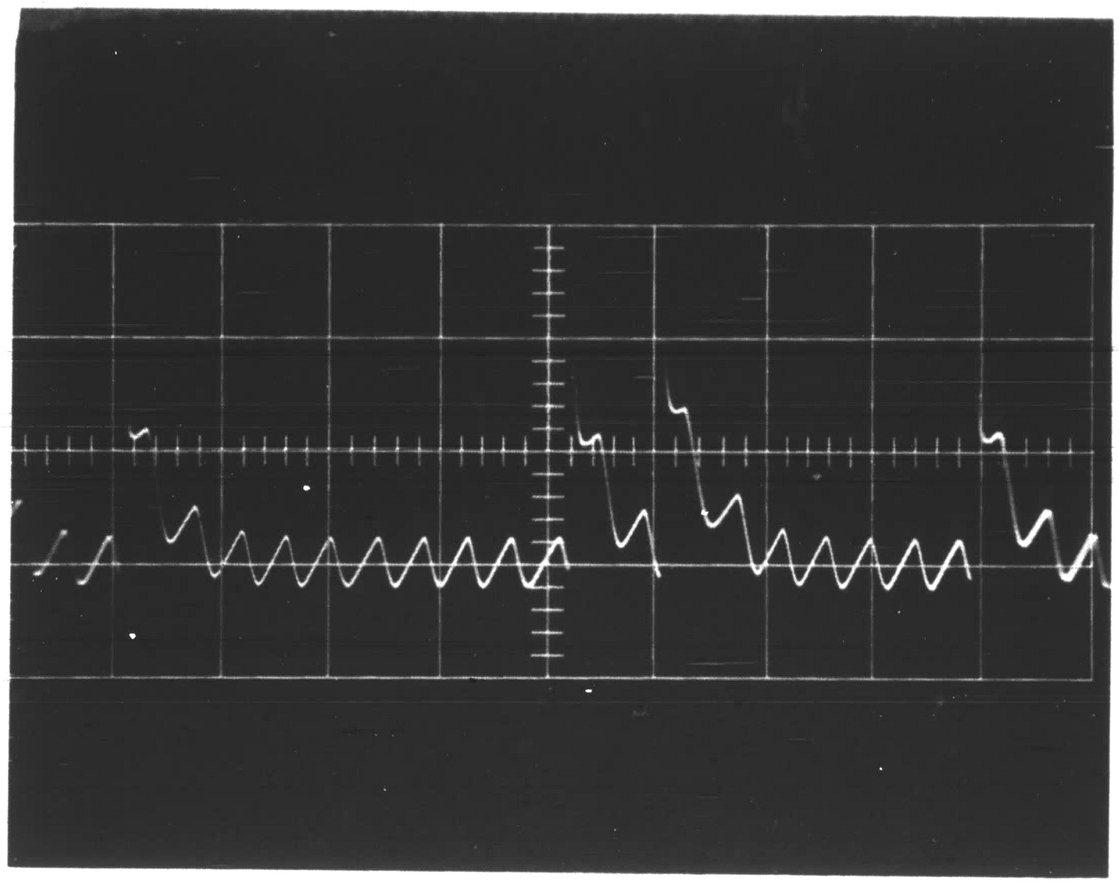

Figure 9. Voltage wave form with SCR circuit. Vertical base 50v/cm, time base 20ms/cm.

introduction of this circuitry into the machine influenced the servo system circut and all experiments were performed under manual control of the electrode feed.

An Anadex model CF-250 portable counter was used to total the number of pulses of over 20V magnitude. The response of this unit was sufficient to discriminate pulses with a frequency of 10^{-5} seconds. The Agietron was not capable, in the modified condition, of pulsing more frequently than every 20 milliseconds. Figure 10 shows the wave form of the circuit with the final modification.

Calorimeter

A stirring type calorimeter (Figure 11) was designed and made from $\frac{1}{4}$" plexiglas to measure the thermal energy expended as a result of the machining process discussed later in this paper. A chromel-constantan thermocouple was calibrated against a Bureau of Standards Certified Thermometer and used to determine temperature changes in the

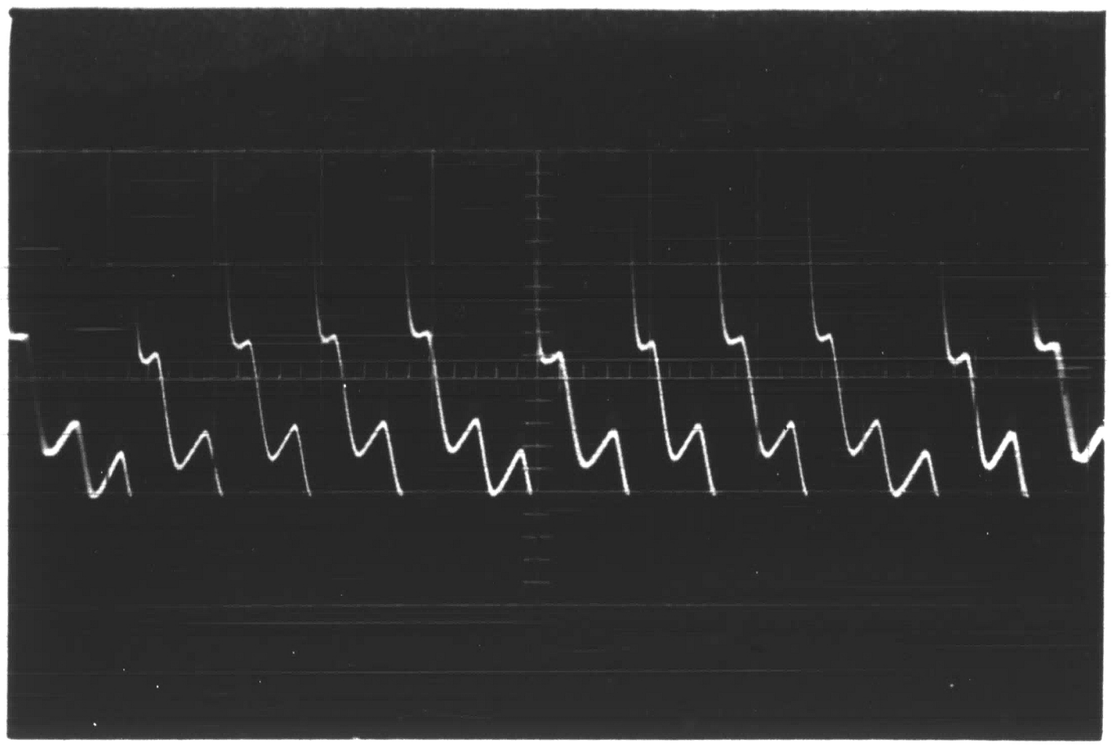

Figure 10 Voltage wave form with SCR clipped circuit. Vertical base 50v/cm, time base 20 ms/cm.

calorimeter. The thermocouple output was amplified 100X using the DC amplifier in a Model 95A Boonton Voltmeter. The DC amplifier output was fed to a Houston Instrument Corporation, Model HR-97 X-Y Recorder which was calibrated with a D-C source of known voltage.

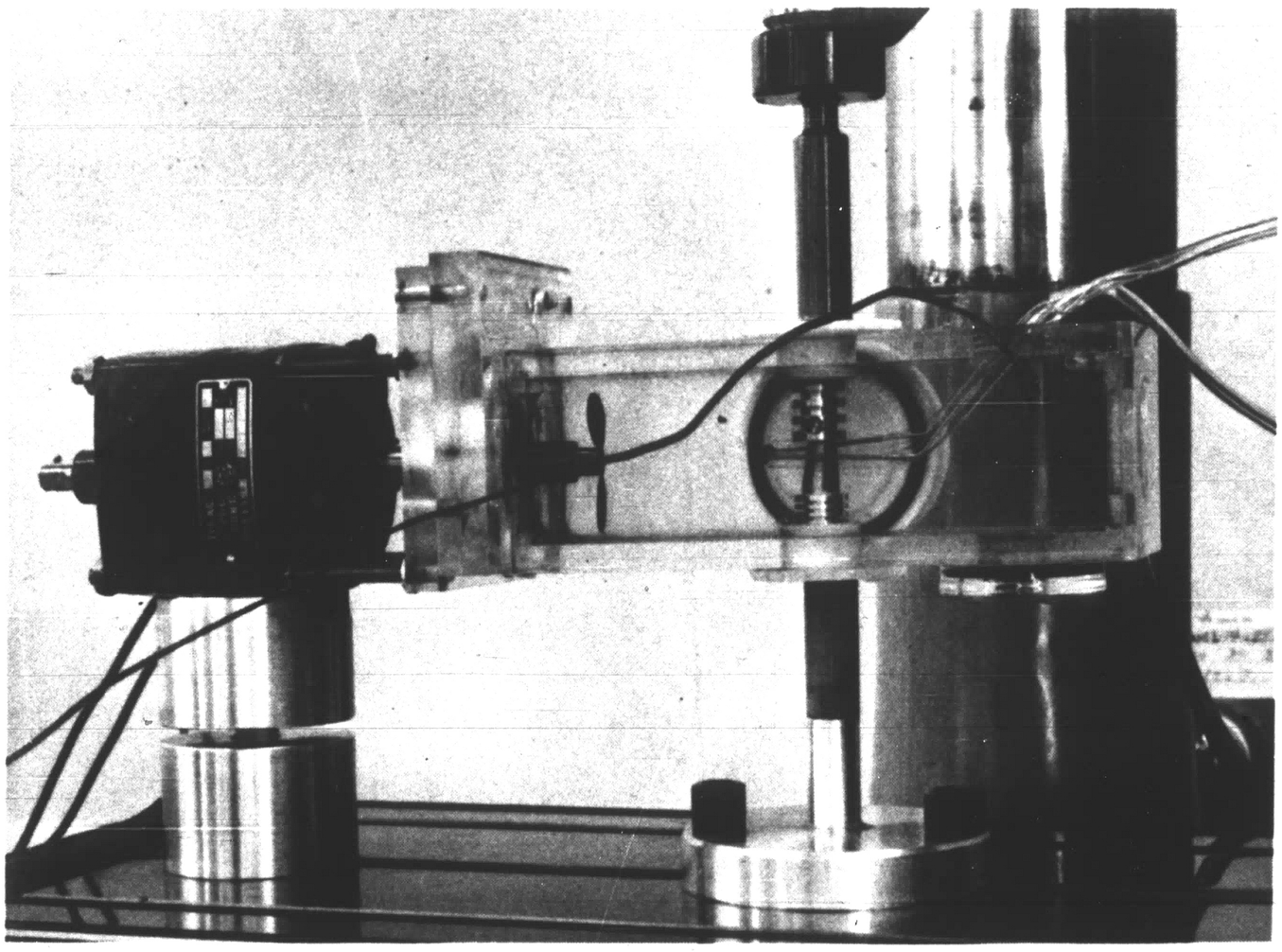

Figure 11 Calorimeter

Materials Used

The choice of materials for anode and cathode were, for the most part, made without regard to commercial application of the results. Yellow brass rod stock of composition 61.50% Cu, 35.25% Zn and 3.25% Pb was chosen for the cathode on the basis of availability.

The anode material selected was beta-tin, a body centered tetragonal material with lattice parameters of a = 5.8311 c = 3.1817 at 20°C (7). Single crystals, 1/4 inch diameter, 1/2 inch long, with growth axes in the [100] and [001] orientations were purchased from Semi Elements Company, Saxonburg, Pennsylvania and Harshaw Chemical Company, Cleveland, Ohio and assayed spectrographically at 99.9947% tin with traces of silver and bismuth. Crystal designations H and SE, to represent the suppliers, followed by a number (e.g. H001-1) to represent the growth axis orientation and crystal number, were assigned to the material as it was received.

The choice of a body centered tetragonal lattice was directed by considerations of simplicity of structure with extremeness of lattice parameter and ease of computation of nearest and next nearest neighbor distances. This was the only element meeting the above criteria having stability at room temperatures. The anisotropic qualities of tin are extreme, thus it was felt that of all the materials considered for this study, tin would tend to give the best discrimination between data obtained from the extreme orientations. Barrett (9) gives the properties for beta tin, shown in Table I, in the orientations used in the study.

Table I

Some properties of beta tin single crystals

	[001]	[100]
Electrical Resistance, 10^{-6} ohm-cm	14.3	9.9
Thermal Expansion, 10^{-6}	30.5	15.5

The dielectric medium used in the machine was a proprietary compound called Solvasol #6 sold by Mobile Oil Company. Solvasol is a hydrocarbonaceous distillate which contains, by volume, 41.5% Napthenes, 35.4% Paraffins, 0.3% Olefins and 22.8% Aromatics, and has a specific gravity of 0.7862 at 20^{o}C, a Boiling Point of 437^{o}F and a closed Flash Point of 145^{o}F.

Results and Discussion

Results

Table II shows initial data taken after the SCR circuit was designed and installed in the Agietron.

Observing each day's data as an entity, it can be resolved that the amount of material removed per pulse increases with dielectric temperature. This might be explained on the basis that:

1. Atom to atom bonding becomes weaker as temperature increases due to greater amplitude excursions about their mean lattice position, or
2. As temperature increases the dielectric constant decreases and less energy is required to break down or ionize the fluid.

The temperature rise of the dielectric during a series of runs on a given day was caused by the friction work of the pump mentioned earlier. Subsequent data were taken after the pump had been allowed to run continuously overnight or until the dielectric reached an equilibrium temperature which was 49°C in a 23°C ambient atmosphere.

With the dielectric temperature equilibrated, the results shown in Table III were obtained.

Since the data in Table III had a range of less than 3% for the [100] and [001] orientations, it was felt at this time that the experimental technique had been mastered and the circuit refined to an extent that reproducibility was assured.

To determine the magnitude of the energy involved, a sample calculation was made using for 25,000 pulses, a capacitance (C) of 1.39 micro-

Table II

Data showing the effect of dielectric temperature rise on material removed per pulse.

Date	Run	Dielectric Temperature	Material Removed Micrograms/Pulse
1-14	1	28 °C	0.8284
	3	34	0.8459
	4	37	0.8625
1-15	7	37	0.8070
	9	44	0.8747
	10	47	0.9041
1-17	14	28	1.0712
	15	31	1.0858
	16	34	1.1358
	17	38	1.1620
1-21	18	27	1.0464
	19	32	1.0724
	20	38	1.0776
	22	44	1.1100
	23	45	1.1112

Machine settings: V5, J1, C5

Crystal used: SE 100-1

Table III

Constant Dielectric Temperature Data

Run	Orientation	Microgram/Pulse	No. Pulses
26	100	1.0848	25,001
27	100	1.0532	25,001
28	100	1.0720	25,005
1	001	1.0707	25,002
2	001	1.0540	25,005
3	001	1.0600	25,005
4	001	1.0408	25,004
5	001	1.0440	25,006

Machine settings: V5, J1, C5

Crystals used: SE 100-1, SE 001-1

Dielectric Temperature: 49°C

farads and a voltage (V) 150 volts. The total energy (W_T), the energy stored in a capacitor times the number of discharges or pulses, is

$$W_T = \tfrac{1}{2} CV^2 \text{ x no. of pulses}$$

$$= \tfrac{1}{2}\ 1.39\ (10^{-6})\ (150)^2 \text{ x } 25\ (10)^3$$

$$= 392 \text{ joules}$$

or multiplying by .239 cal/joule

$$E = 93.4 \text{ cal}$$

An Energy Balance

Although the total energy for 25,000 pulses is seen from the

above calculation to be on the order of 90 cal, this cannot be considered all anode or workpiece erosional energy.

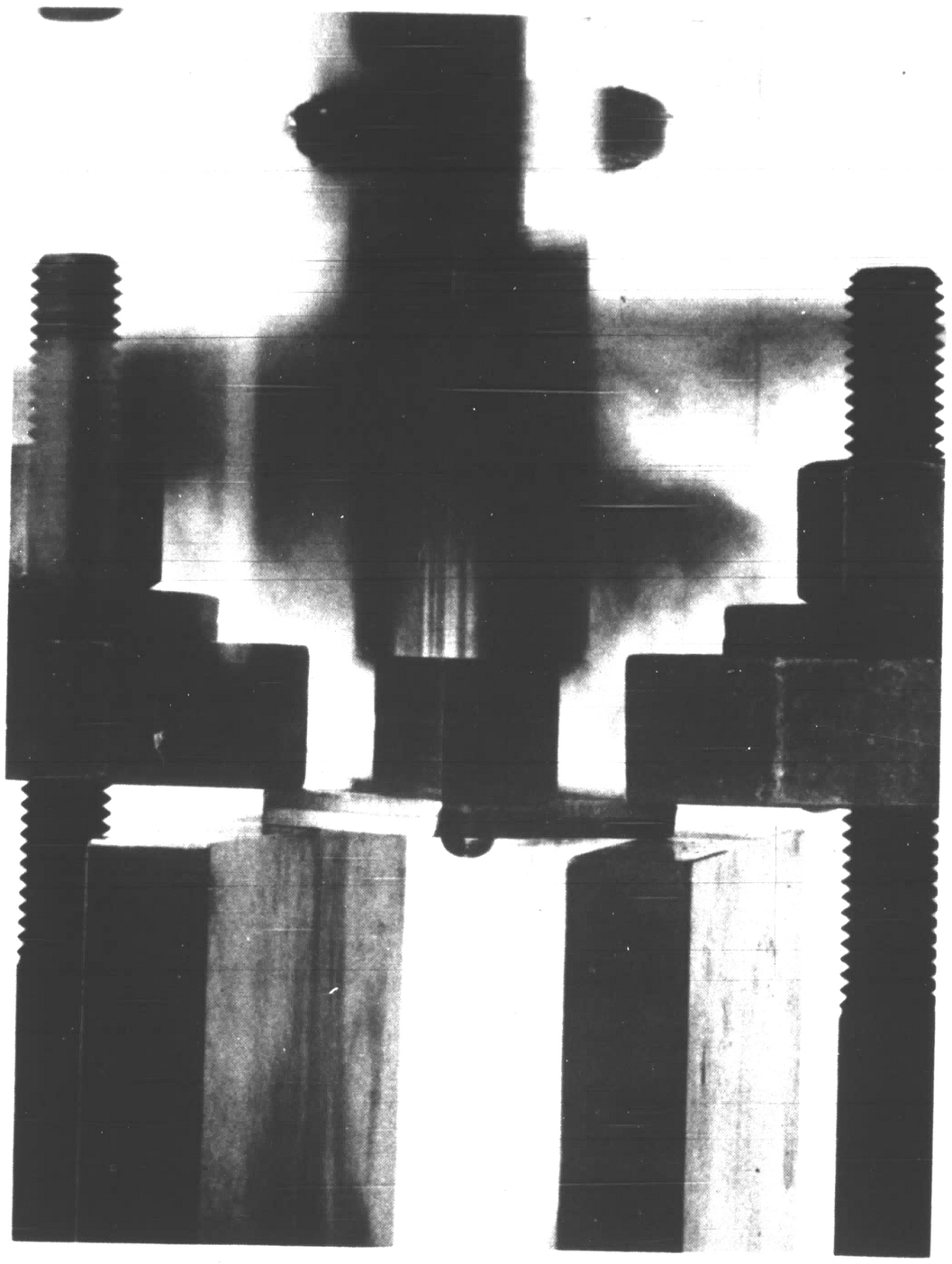

Figure 12. The gap during machining showing the carbon cloud and released gases.

Figure 12 shows some of the phenomena occurring in the gap during machining. Two phenomena shown in this picture are the release of carbon and the formation of gas from the dielectric. Other energy losses that could be considered are: sonic, radiation, and tool or cathode erosion. One might also speculate on the energy required to initially bridge the gap and an energy loss associated with alignment of the dielectric molecules if a polar fluid were

used. Undoubtedly, there are also other thermal losses, for instance, the I^2R losses in both tool and workpiece and the leads due to the currents passing through each. In summing up these energy losses, lumping many of them in a W_x term,

$$W_T = W_E + W_{Th} + W_{l-g} + W_{g-s} + W_x$$

where W_T = Total energy as determined from the pulse count and charge held by the capacitor

W_E = Erosional energy

W_{Th} = Thermal energy in the dielectric temperature rise due to machining

W_{l-g} = Thermal energy required to produce a vapor from the fluid or the chemical energy required to produce a lower or higher molecular weight gas from the fluid

W_{l-s} = Chemical energy required to produce carbon plus a fluid of different molecular weight and composition from the distillate used.

W_x = Energy due to I^2R losses, sonic losses, alignment losses, etc.

It was thought that if an energy balance could be made, W_E, the erosional energy could be determined.

The calorimeter mentioned earlier was used to measure the thermal energy rise W_{Th} of the fluid but the apparatus was not sensitive enough to detect less than 25 cal/10 minute input through a $\frac{1}{2}$ watt resistor.

The liquid-to-gas (W_{l-g}) and liquid-to-solid (W_{l-s}) energy losses could have been determined if a complete chemical analysis in

terms of the component molecular weights of the liquid before machining and the gas and liquid after machining could have been performed but the facilities for such analysis were not available.

It was decided at this time to assume that the energy balance components other than W_T and W_E, the total and erosional energies, would be constant and independent of crystal orientation. Under these assumptions

$$W_T = W_E + \text{Constant}$$

W_T for the [100] and [001] orientation could be compared and if a difference was evident it could be concluded with reasonable confidence that the erosional energy, W_E, was truly different.

The effect of dielectric temperature

Table IV shows the results obtained in machining two crystals of different orientations at 49°C and 25°C. These data again show a fairly strong temperature dependence, but at both temperatures the scatter about the mean is so great (Figure 13) that a determination of energy as a function of temperature from these data would be worthless.

The effect of pulse rate, gap variation, and dielectric contamination.

Further analysis of the results from the data shown in Table IV revealed a dependence between micrograms/pulse and the time required to pulse 10,000 pulses or in other words the weight of material removed depended on how fast the pulses occurred. This observation resulted in the addition of the clipping diodes mentioned on page 17 which restricted the maximum charging voltage to 152V. It was felt that this rate dependence could be reasoned as follows:

Table IV

Results from machining two crystals of different orientations at two dielectric temperatures.

SE 001-1				SE 100-1		
T^oC	Run	Micrograms/ Pulse	Time Min.*	Run	Micrograms/ Pulse	Time Min.*
49	6	1.178	16	29	1.128	17
	7	1.213	13	30	1.229	13
	8	1.137	20	31	1.133	15
	9	1.126	12	32	1.160	12
	10	1.204	10	33	1.142	10
25	11	0.892	13	34	0.908	15
	12	0.913	13	35	0.871	16
	13	0.912	18	36	0.968	15
	14	0.905	10	37	0.879	11
	15	0.866	9	38	0.901	10
	16	0.909	10	39	0.909	12
	17	0.842	11	40	0.896	12
	18	0.978	11	41	0.913	13
	20	0.885	13	42	0.967	9

Machine Settings: V5, J1, C5

* For 10,000 discharges

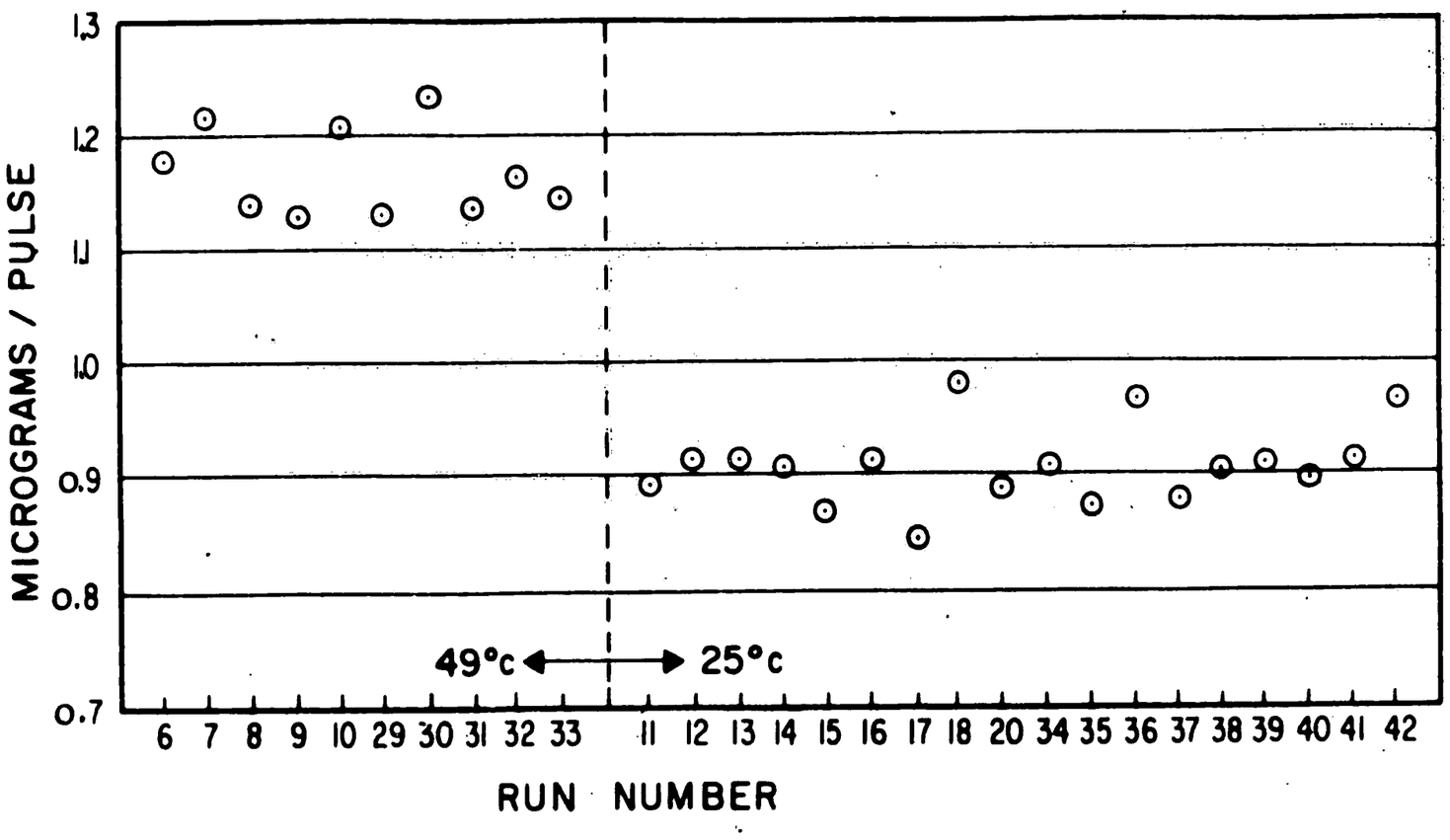

Figure 13 Results from Table IV

1. When machining at a slow pulse repetition rate which is reflected in the time it takes to pulse for example 10,000 times, the gap must of necessity be held at nearly its maximum separation. Under these circumstances one or all of the following three effects could be influencing the specific material removal.

a. Since the gap is at the maximum separation for one spark discharge, it may be over the maximum for the next discharge to occur because the metallic asperity on which the first discharge initiated or to which the first discharge proceeded may have been eroded by that discharge. If it is over the maximum and it is necessary to reposition the electrodes to provide for another discharge, the probability that it will occur at a voltage higher than 150V is greater. This would result in greater material removal/pulse.

b. Since the gap is at maximum separation, there is a greater thickness of dielectric between the electrodes, hence when a discharge occurs, the energy balance might change so that more energy is needed to break down the dielectric and less energy is available for erosion, so that less material is removed per pulse. Barash (2) has postulated that the proportion of energy losses in the gap is proportional to separation.

c. Since the gap is at a maximum and the discharges are occurring less frequently, there is better removal of eroded particles. This would mean a cleaner and higher effective dielectric constant fluid in the gap. The result of this would be as in (b) above with less material removed/pulse.

2. When machining at a fast rate or at a gap separation of less than required for the voltage being used

a. The pulses will probably be of minimum voltage

b. The dielectric layer is thinner and requires proportionately less energy to ionize it and

c. The effective dielectric constant will be lower due to inefficient removal of eroded material.

After the clipping diodes were added to eliminate any overvoltage, a designed experiment was run to determine if the rate dependence was a circuit or gap parameter. The data are shown in Table V. Figure 14 shows the dependence found between material removed and time to pulse 5,000 times.

Table V

Results of the Designed Experiment to determine the cause for pulse rate dependence.

Orientation & Run	Time, secs for pulse count					Material Removed, Milligrams	*
	1000	2000	3000	4000	5000		
001-5	15	40	80	140	195	8.80	S
001-6	75	140	195	225	380	7.34	S
001-7	10	23	38	60	82	8.98	F
001-8	13	26	40	60	81	8.90	F
100-5	65	125	187	235	291	7.84	S
100-6	70	177	260	303	346	7.29	S
100-7	27	45	66	84	102	8.89	F
100-8	10	24	40	60	76	9.84	F

Machine Setting: V7, J1, C5
Crystals: H 001-4, H 100-2
Dielectric Temperature: 24°C
*Attempted manual control of pulse rate: F - fast, S - slow

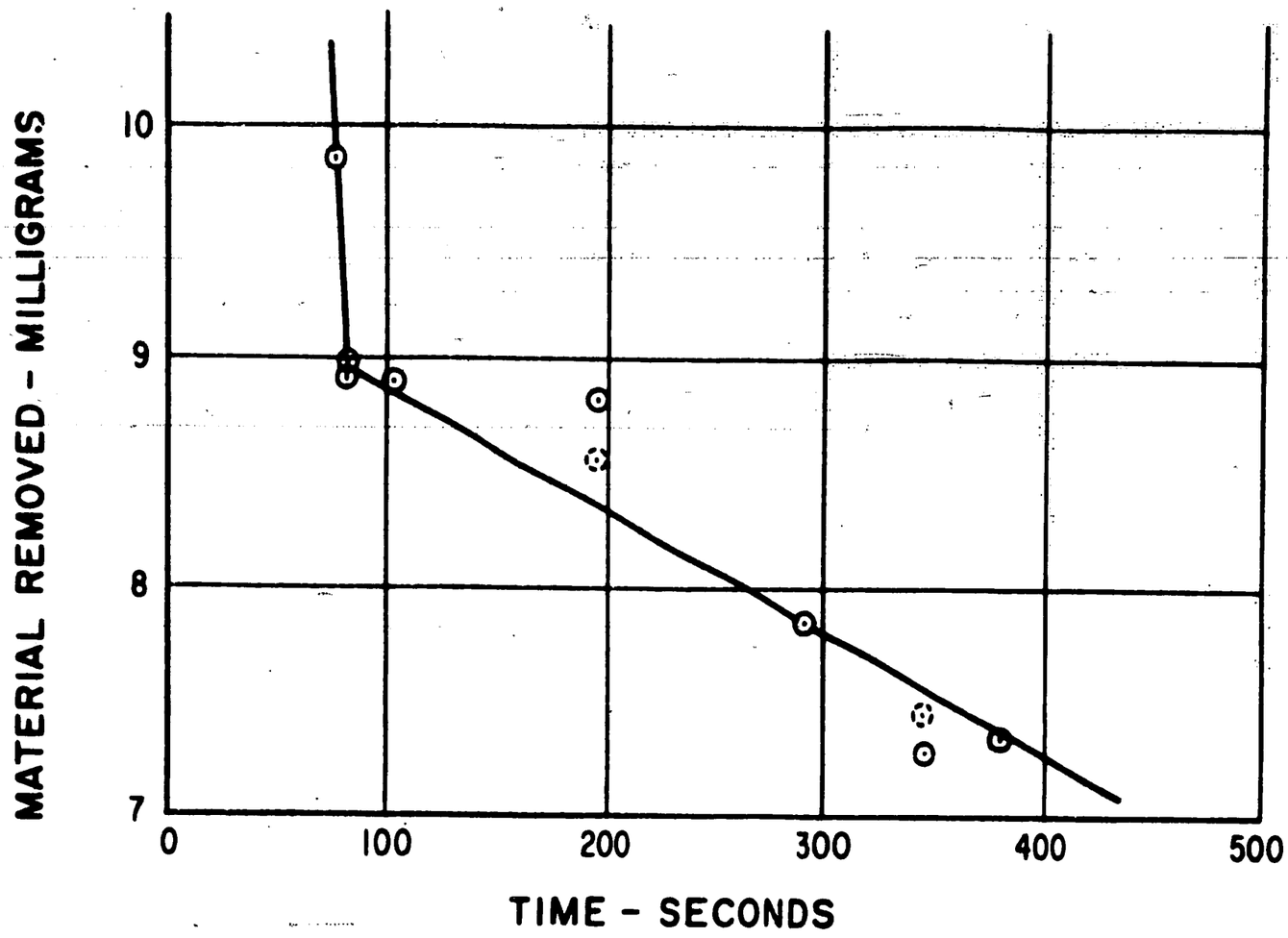

Figure 14. Material removal rate from data of Table V.

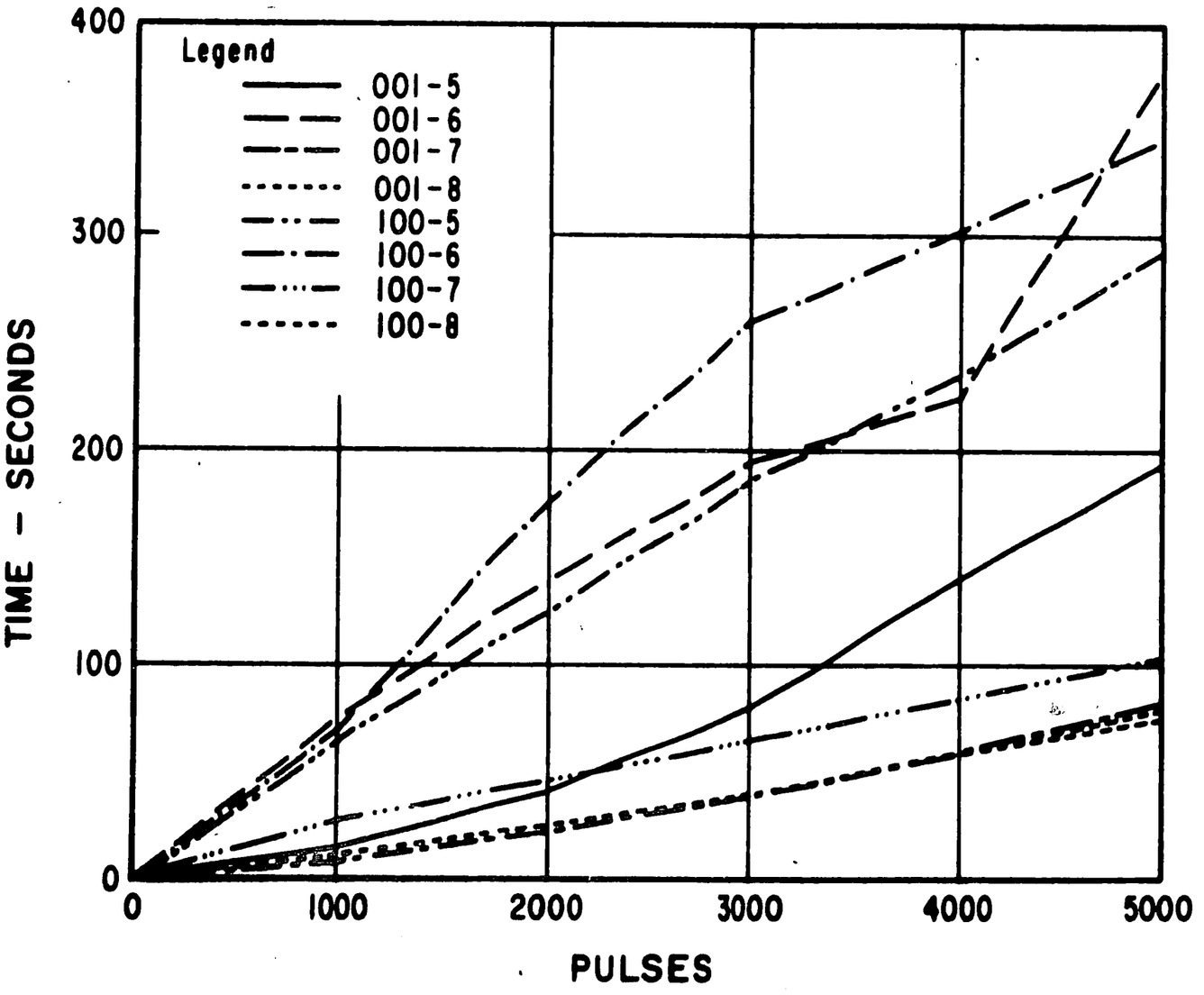

Figure 15. Pulse rate from data of Table V.

Figure 15 shows pulse versus time data from Table V. It can be seen that except for runs 100-6, 001-6 and 001-5, the pulse rate is approximately linear. Since the above runs were conducted at various rates, it was decided to apply a weighted correction based on rate to these data to determine if a function could be better defined.

Considering run 001-5 where material removal was 8.80 mg

Counts	Time Seconds	Δ Time Seconds	5Δ	mg From Fig. 14
1000	15	15	75	10.00
2000	40	25	125	8.75
3000	80	40	200	8.35
4000	140	60	300	7.80
5000	195	55	275	7.95
				42.85 Ave.
				8.57 mg.

The milligram vs. time functional curve was defined (Figure 14) using only the data points having linear pulse rates as determined from Figure 15. The non-linear pulse rates were broken down, as in the above example into five segments of linear pulse rates and multiplied by five. The material removal at this pulse rate was obtained from the assumed function on Figure 14 and averaged. The dotted data points on Figure 14 show the non-linear runs as if they had been constant pulse rate data.

Functional Curve Theories

Two theories for the discontinuous nature of the above functional curve are postulated.

Gap and Contaminant Theory

When machining in the region defined by the small negative slope, as the pulse frequency is increased (or the time to pulse 5000 pulses is decreased) the electrodes are at a gap separation less than that required for the voltage applied hence less energy is required for dielectric breakdown or spark channel formation and more energy is available for erosion. The ionization energy is inversely proportional to gap separation. In this region the frequency is sufficiently slow and the gap is adequate that particle removal is relatively effective.

b. In the region of the steep negative slope, the gap is so narrow that scavenging is inefficient and the dielectric becomes so contaminated with a subsequent decrease in dielectric constant that an extremely small amount of energy is required for spark initiation.

Spark-Arc Theory

In the small negative slope region of the functional curve, the mode of erosion is by spark alone. At the break-over point the erosion is principally effected by an arc discharge. This is a condition in which the sparking frequency is of sufficient magnitude such that the discharge column does not fully collapse before the following spark is programmed. This condition would practically negate spark initiation energy losses and would result in more energy available for erosion.

The effect of surface polycrystallinity

It was observed by the Laue back reflection method, Figures 16 through 19, that the surface of each orientation of single crystal after machining showed Debye ring formation and spot smearing.

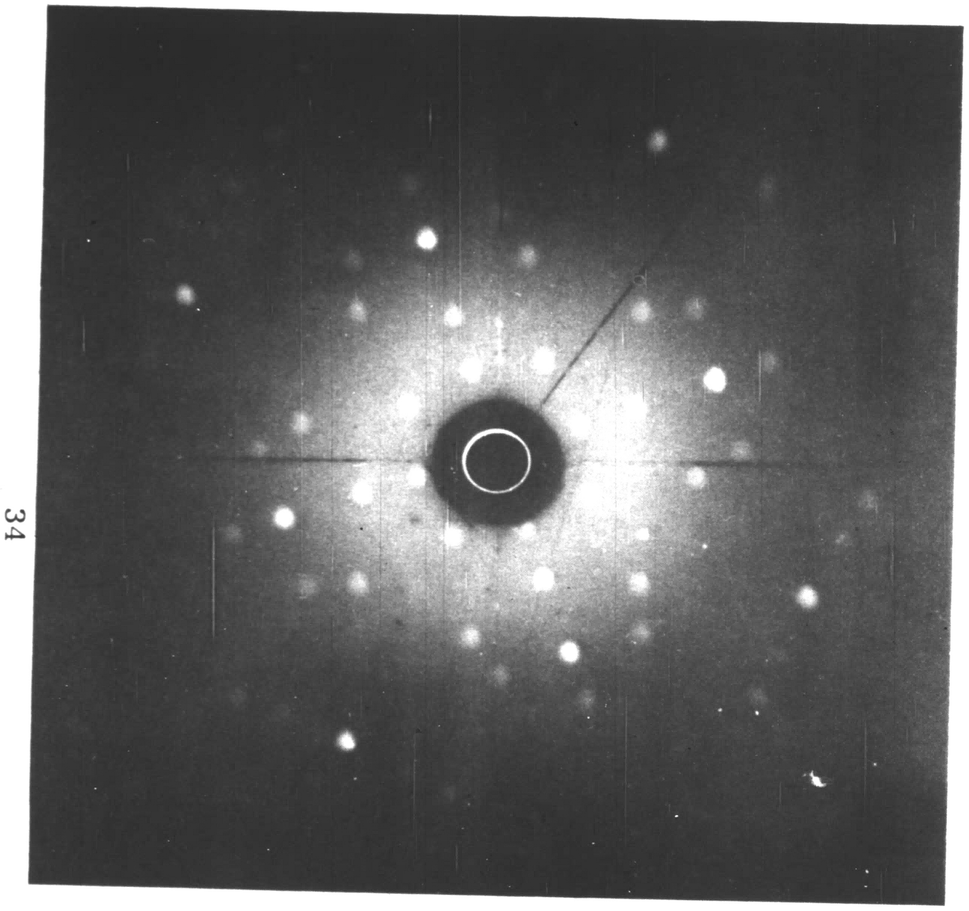

Figure 16 Laue method X-ray of crystal H001-4 before machining.

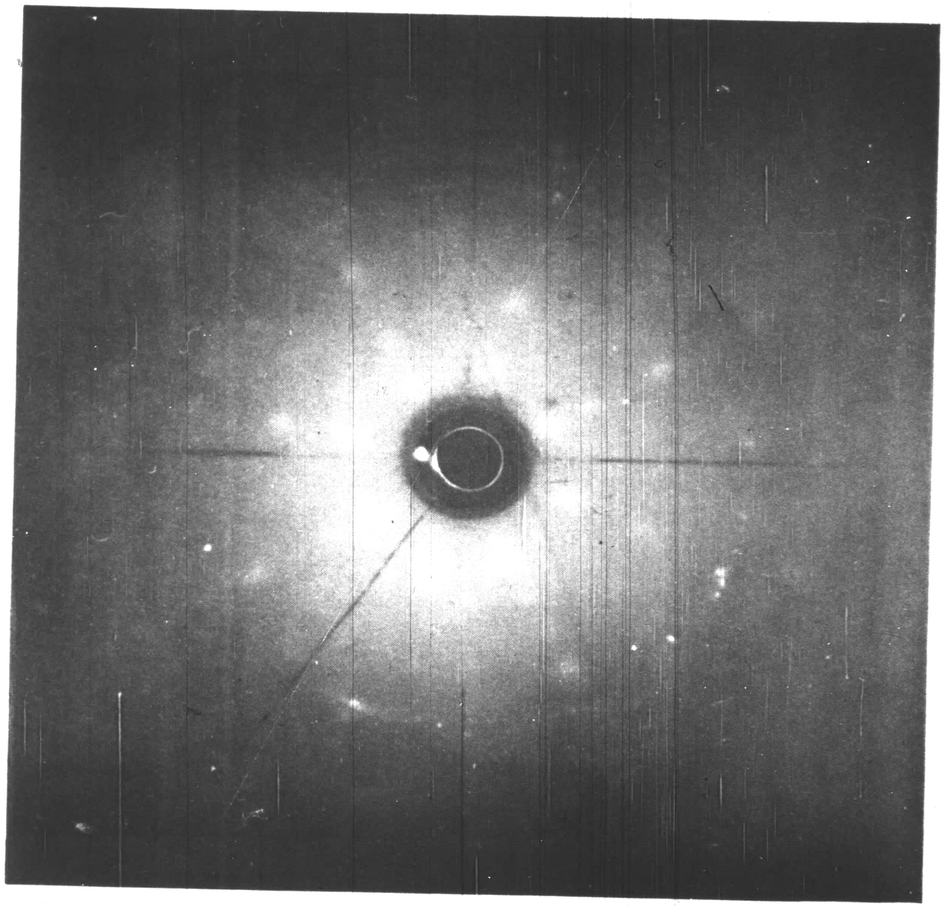

Figure 17 Laue method X-ray of crystal H001-4 after machining.

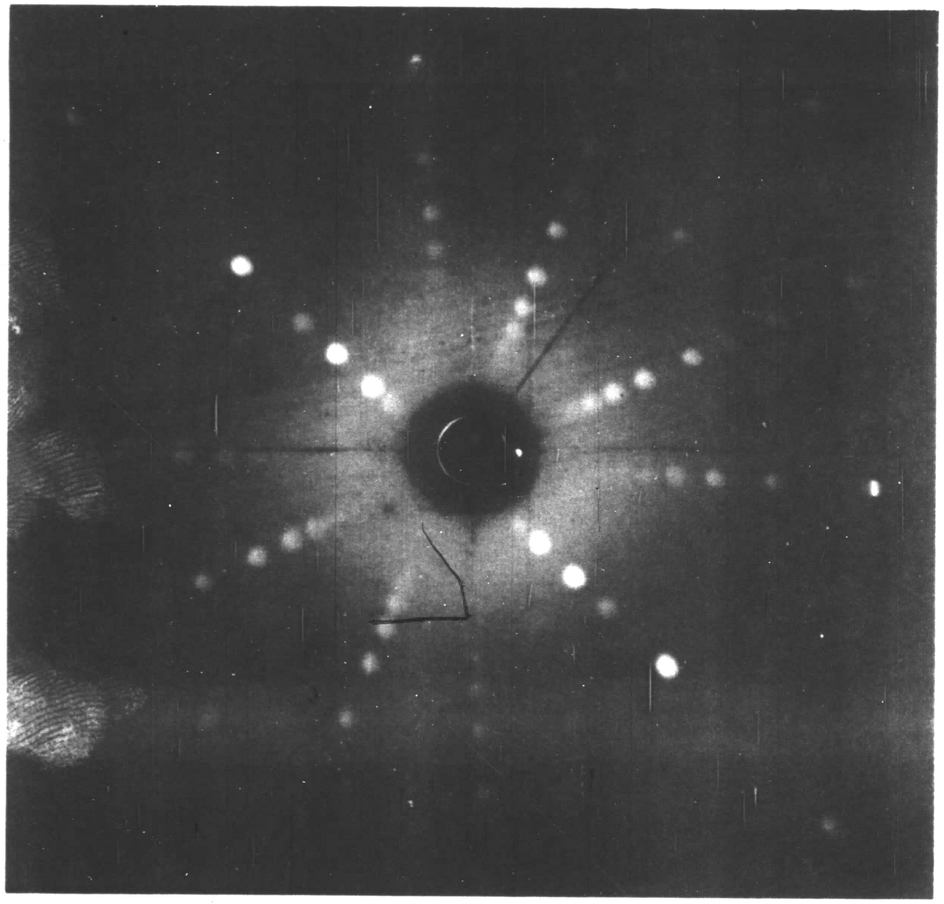

Figure 18 Laue method X-ray of crystal H100-1 before machining.

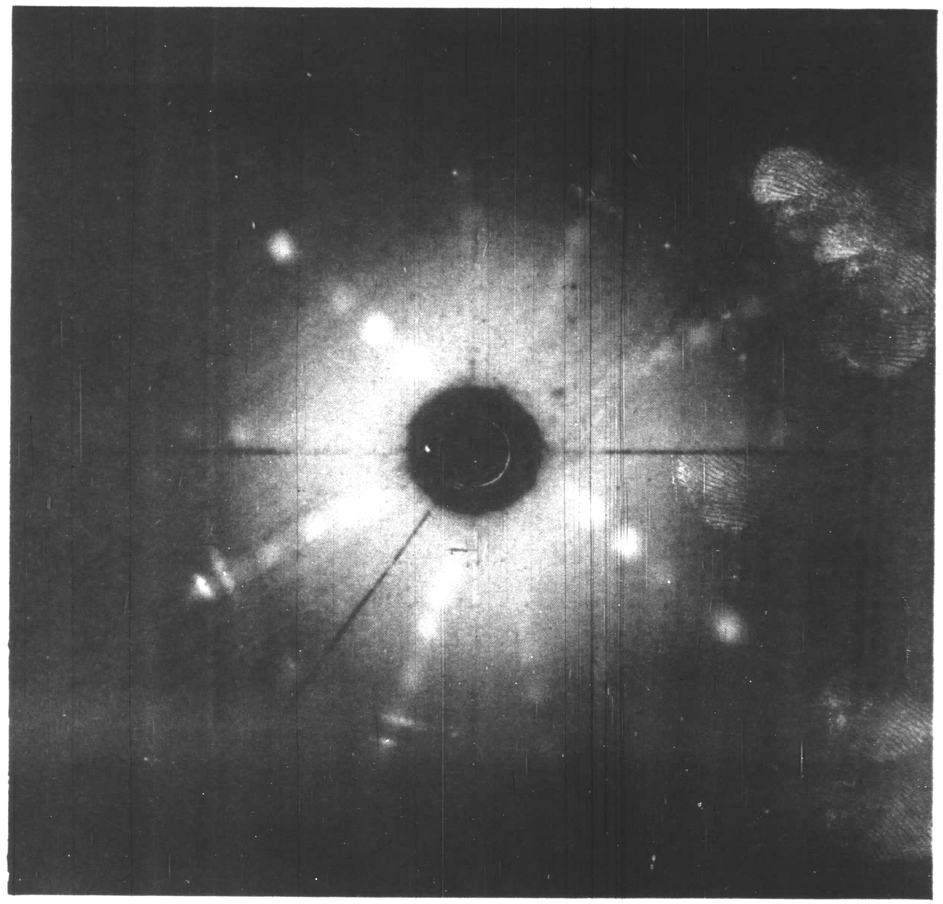

Figure 19 Laue method X-ray of crystal H100-1 after machining.

These are indications of polycrystallinity and lattice strain.

The depth of penetration of Cu Kα in beta-tin is about 12 microns assuming a ratio of exit to entrance beam intensities of 1:10. This might indicate that the damage to the single crystal by the EDM process is more than a slight surface rearrangement of atoms. Electron diffraction of the machined surface revealed polycrystalline copper deposits presumably from the brass electrode (Figure 20a). This finding is similar to the mention by Opitz (3) of a layer of copper on pure iron after electrodischarge machining with a copper tool and Cole and Grigson (10) who found a thin polycrystalline layer on molybdenum.

The copper deposit was removed (Figure 20b) and spotty Debye rings indexed to be beta-tin were discovered.

Figure 21 shows etch markings along [001] direction on the surface of a [100] crystal which had been electro-discharge machined. Similar [100] and [001] slip or dislocation lines have been shown on the surface of [100] tungsten crystals after electro-discharge machining by Mueller and Wadewitz (11). Sestak and Libovicky (12) recorded observations of plastically deformed areas and dislocation lines in a high purity Fe - 4% Si alloy after electro-discharge machining.

Figure 22 shows typical craters in a 2:1 sectioned tin single crystal. Average crater depths of 15 microns are measurable.

Figure 23 shows etch markings on a 2:1 sectioned crystal extending through the surface from 150 microns deep and etch markings 250 microns below the crystal surface. These etch markings could be twins which have been observed in beta tin by Chalmers (13).

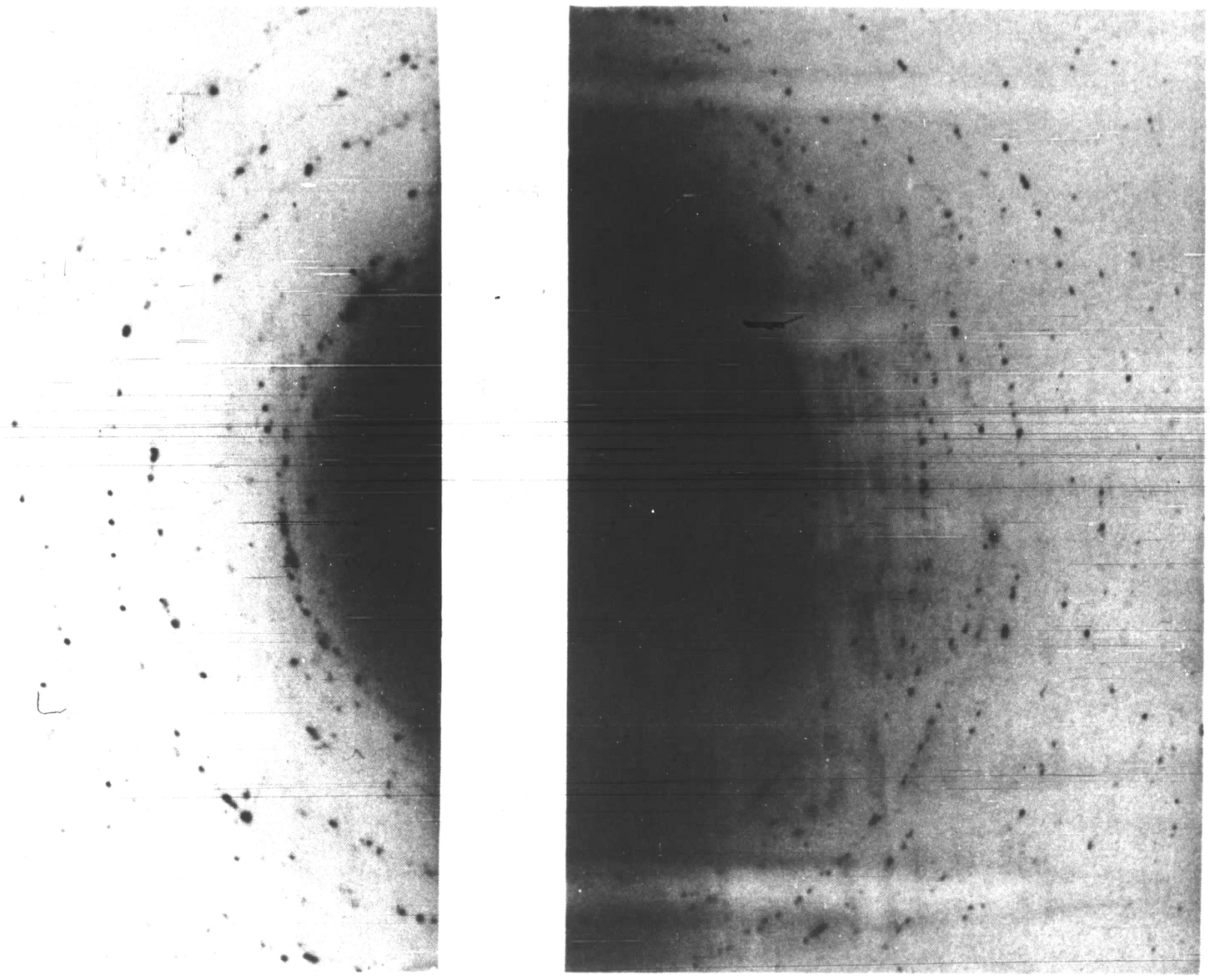

(a) (b)

Figure 20 Electron diffraction of electro-discharge machined surface of beta-tin crystal showing
a. polycrystalline copper deposit
b. polycrystalline tin after copper was removed by etching

Figure 21 Etch markings on surface of [$\bar{1}00$] beta tin single crystal after EDM, HNO_3 : distilled water :: 1 : 1 etch (200X)

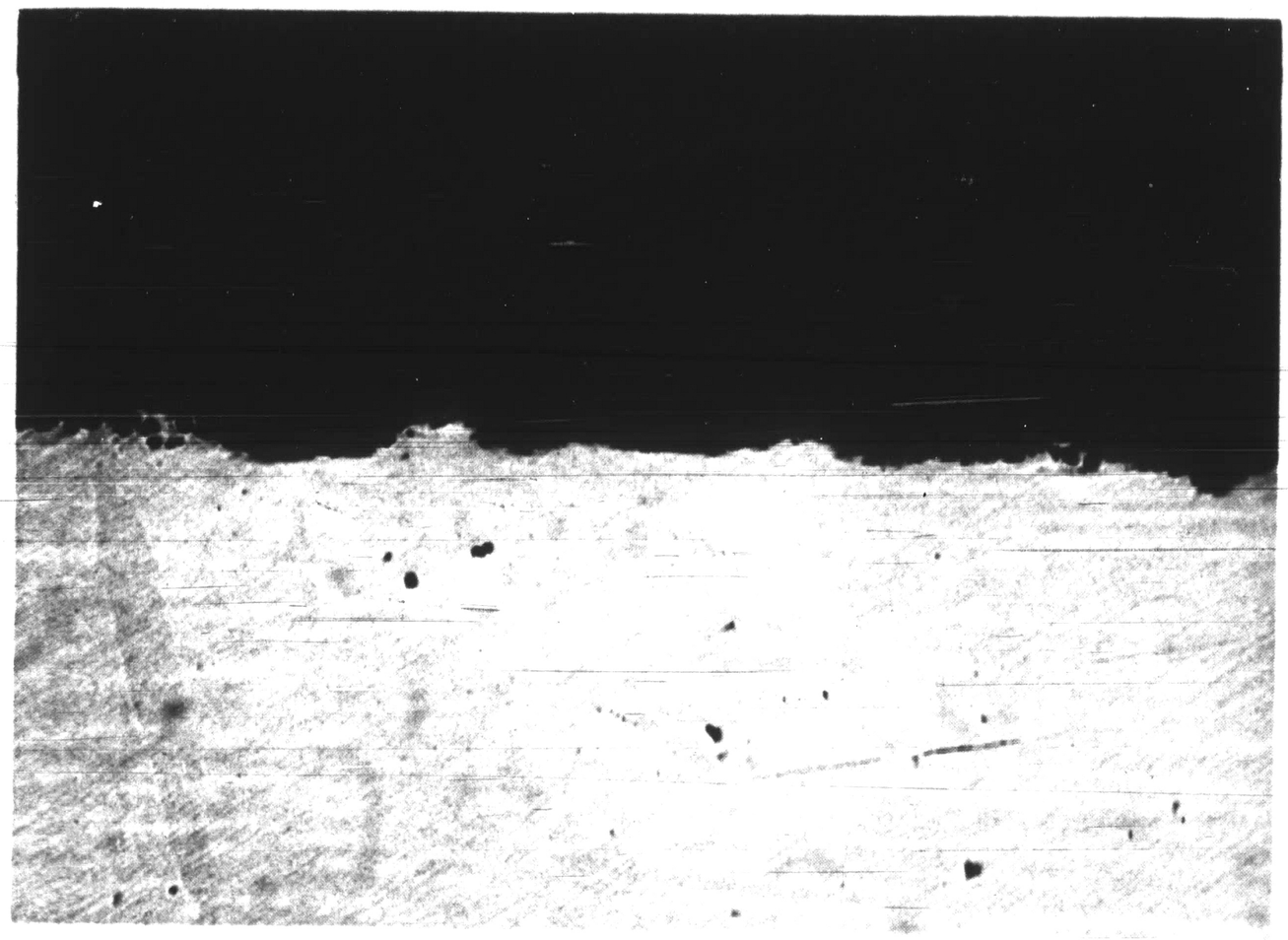

Figure 22 Typical surface craters as a result of EDM on a 2:1 sectioned beta tin single crystal (50X)

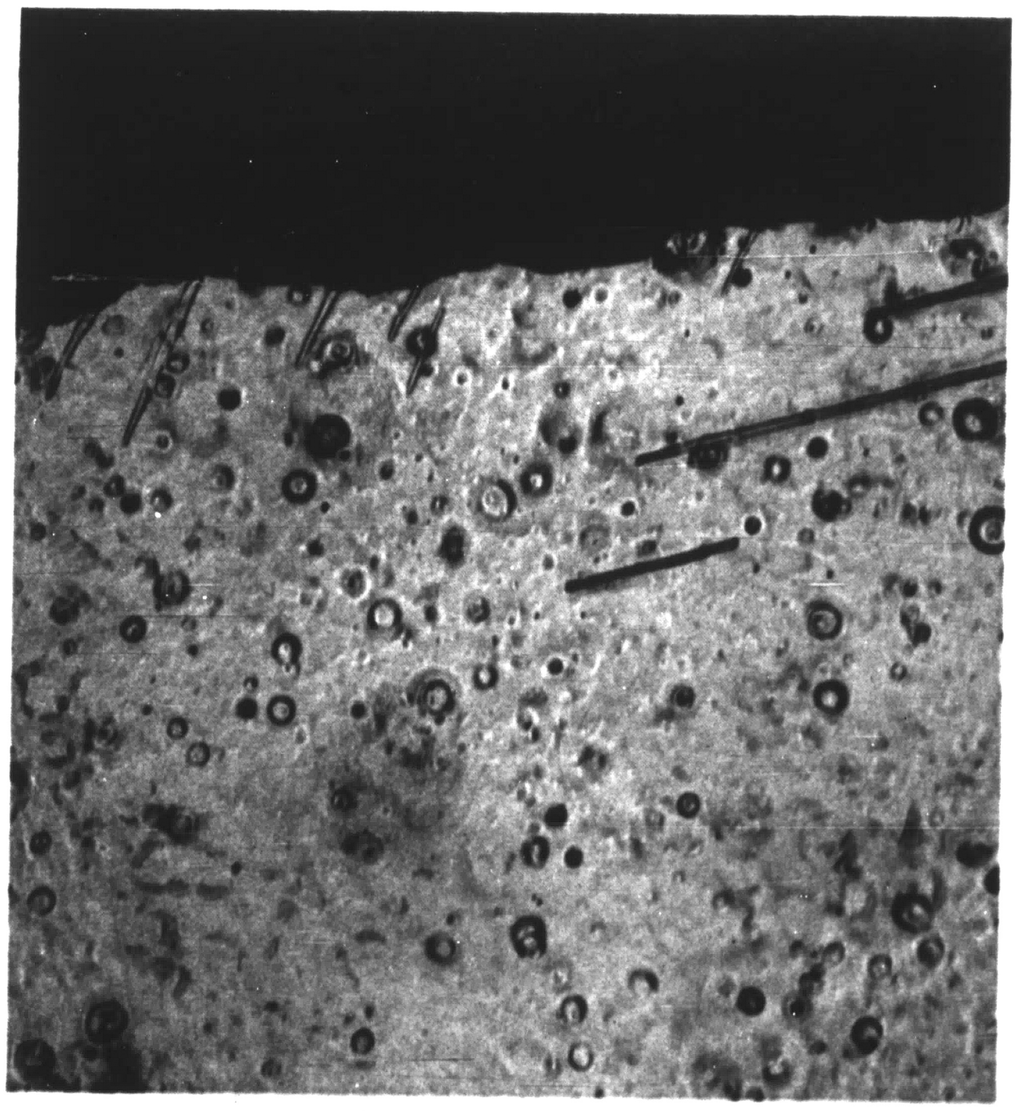

Figure 23 2:1 sectioned crystal showing etch markings: HNO_3 : distilled water : : 1 : 1 etch (50X)

Figure 24 shows the same sectioned surface with a polycrystalline layer 12.5 microns thick on the single crystal substructure.

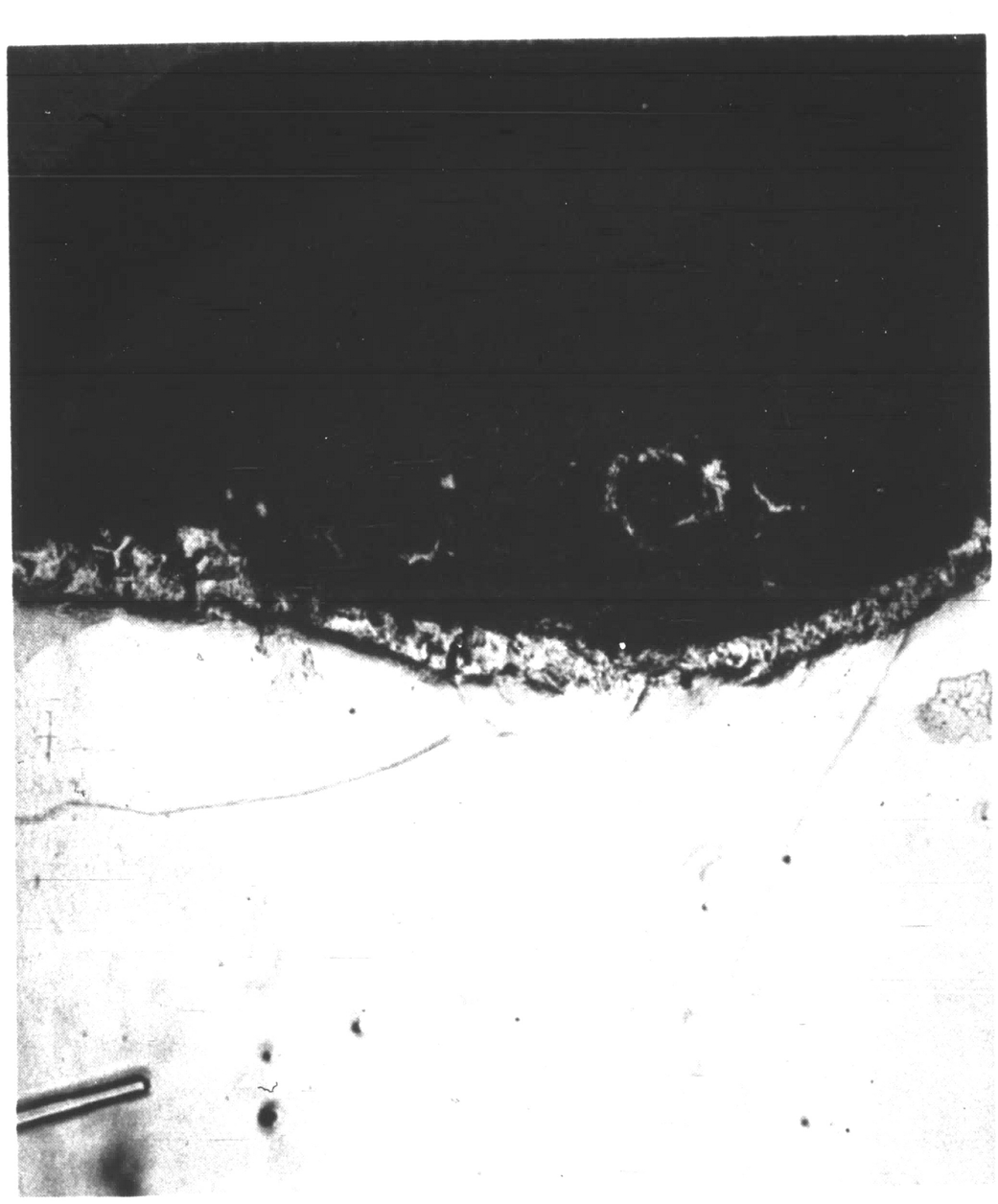

Figure 24. 2:1 sectioned crystal showing a polycrystalline layer. HNO_3:distilled water::1:1 etch. (200X)

Conclusions

Modification of basically a resistance-capacitance EDM machine, by the inclusion of an SCR controlling circuit, resulted in a method of measuring the relative total energy required to electro-discharge machine a material.

The single crystal material was machined in two orientations and the relative energy per unit weight of material removed was determined. It is felt that a comparison of energies required to erode two different crystallographic orientations in a single crystal by a commercial electro-discharge machine will not yield confident results because

1. a polycrystalline layer of copper from the brass tool is deposited on the surface being eroded
2. a polycrystalline layer of the tin being eroded is formed on the surface under study
3. the subsurface of the tin crystal being machined is severely deformed and
4. that gap spacing and dielectric contamination cannot be controlled or monitored to any degree of accuracy.

Whether the hypothesis,

$$W \alpha \frac{1}{b^n}$$

that energy is inversely proportional to lattice parameter to some power n, is valid for the electro-discharge machining process cannot be determined by the techniques used in this thesis.

Future Work

To bypass the difficulties encountered in this thesis, it is postulated that an answer to the question of anisotropy of the EDM process could be determined by single sparking of a large area crystal face. It would be necessary to spatially arrange the discharges such that the polycrystallinity produced by one spark did not influence the area selected for the following erosion. It should be possible to completely flush out the gap after each spark and the tool could be withdrawn following each discharge and repositioned by capacitance measurements prior to another discharge.

The development of an effective servo system for gap control could be a significant contribution both to industry and the academic study of the process. A system whereby the between-discharge time is utilized for electrode separation measurement and repositioning would provide a means for optimizing the total cycle efficiency. With the present servo positioning method much machining time is spent in the non-machining mode while the servo hunts for an equilibrium position.

It would be interesting to determine

1. if there is correlation between particle size and crater volume,
2. if the energy per pulse has an effect on the dislocation density,
3. if the particles, which have been spectrographically assayed by the author to contain tin, copper and zinc, are solid solutions, intermetallic compounds or single crystals tin plated with copper and zinc,

4. if the cathode or tool has a polycrystalline layer of the anode material deposited on it during the EDM process, and
5. if the substructure of the cathode is disturbed as the anode was and to what extent.

APPENDIX

A Mathematical Model for Material Removal

Horizontal Bonds

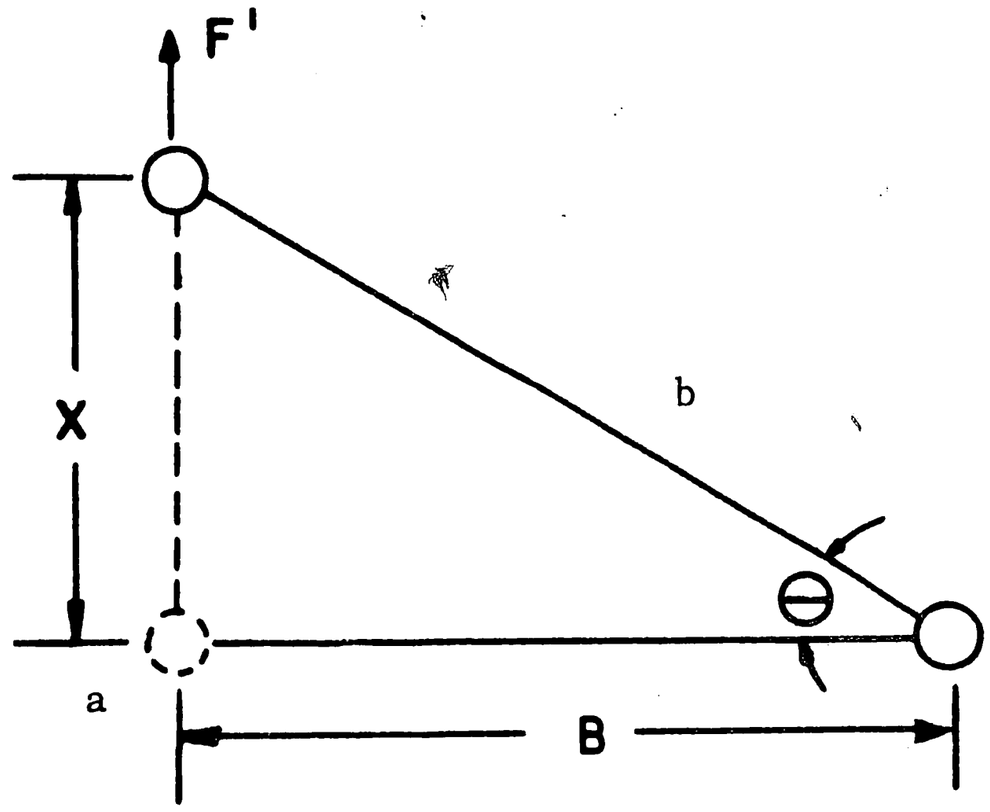

The work or energy, W, necessary to remove atom "a" from its equilibrium position is:

$$W = \int_0^\infty F' \, dx$$

but $F' = F \sin \theta$, then

$$W = \int_0^\infty F \sin \theta \, dx$$

Assuming $F = \frac{K}{b^n}$ where K is a proportionality constant, b is the

bond length and n some exponent ≥ 1.

Then:
$$W = \int_0^\infty \frac{K \sin\theta \, dx}{b^n}$$

but
$$b = \frac{B}{\cos\theta}$$

and
$$b^n = \frac{B^n}{\cos^n\theta}$$

Then:
$$W = \int_0^\infty \frac{K \sin\theta \cos^n\theta \, dx}{B^n}$$

or:
$$W = \frac{K}{B^n} \int_0^\infty \sin\theta \cos^n\theta \, dx$$

since
$$x = B \tan\theta$$

$$dx = B \sec^2\theta \, d\theta$$

then
$$W = \frac{K}{B^n} \int_0^{\pi/2} B \cos^n\theta \sin\theta \sec^2\theta \, d\theta$$

since
$$\sec^2\theta = \frac{1}{\cos^2\theta}$$

then
$$W = \frac{K}{B^{n-1}} \int_0^{\pi/2} \cos^{n-2}\theta \sin\theta \, d\theta$$

Vertical Bonds

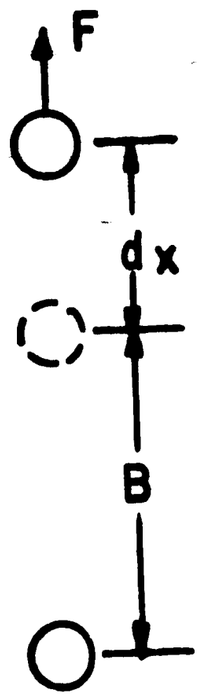

$$W = \int_{B}^{\infty} F \, dx$$

Assuming $F = \frac{K}{x^n}$

$$W = K \int_{B}^{\infty} \frac{dx}{x^n}$$

The evaluation of the above integral will depend on the value of the exponent "n".

Bonds Other Than Horizontal and Vertical

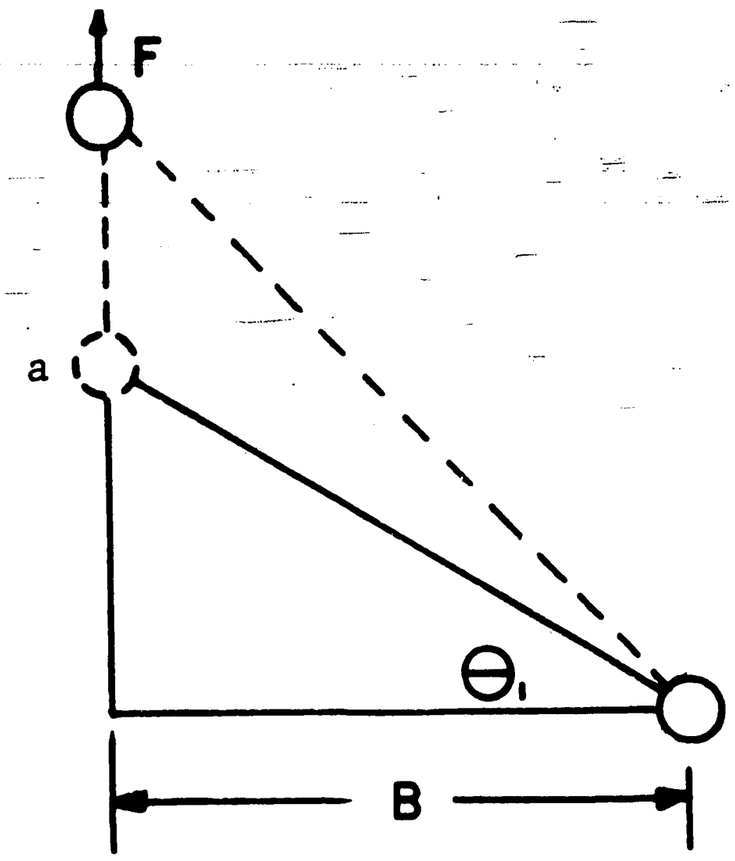

It can be shown that the work required, W, to remove atom "a" from its equilibrium position is similar to that required in the horizontal case but with different limits on the integral.

$$W = \frac{K}{B^{n-1}} \int_{\theta_1}^{\pi/2} \cos^{n-2} \theta \sin \theta \, d\theta.$$

Evaluation of W for n = 1, 2, 3, and 4

Horizontal Bonding

n = 1

$$W = \frac{K}{B^{n-1}} \int_{0}^{\pi/2} \cos^{n-2} \theta \sin \theta \, d\theta$$

$$= K \int_{0}^{\pi/2} \cos^{-1} \theta \sin \theta \, d\theta$$

$$= K \int_0^{\pi/2} \tan\theta \, d\theta$$

$$= -K \left[\ln \cos\theta \right]_0^{\pi/2}$$

$$= K \left[\ln 1 - \ln \theta \right]$$

$$= 6.9K$$

n = 2

$$W = \frac{K}{B^{n-1}} \int_0^{\pi/2} \cos^{n-2}\theta \sin\theta \, d\theta$$

$$= \frac{K}{B} \int_0^{\pi/2} \sin\theta \, d\theta$$

$$= -\frac{K}{B} \left[\cos\theta\right]_0^{\pi/2}$$

$$= \frac{K}{B}$$

n = 3

$$W = \frac{K}{B^{n-1}} \int_0^{\pi/2} \cos^{n-2}\theta \sin\theta \, d\theta$$

$$= \frac{K}{B^2} \int_0^{\pi/2} \cos\theta \sin\theta \, d\theta$$

$$= \frac{K}{B^2} \left[\tfrac{1}{2} \cos^2 \theta\right]_0^{\pi/2}$$

$$= \frac{K}{2B^2}$$

n = 4

$$W = \frac{K}{B^{n-1}} \int_0^{\pi/2} \cos^{n-2} \theta \sin \theta \, d\theta$$

$$= \frac{K}{B^3} \int_0^{\pi/2} \cos^2 \theta \sin \theta \, d\theta$$

$$= -\frac{K}{B^3} \left[1/3 \cos^3 \theta\right]_0^{\pi/2}$$

$$= \frac{K}{3B^3}$$

Vertical Bonding

n = 1

$$W = K \int_B^{\infty} \frac{dx}{x^n}$$

$$= K \int_B^{\infty} \frac{dx}{x}$$

$$= K \left[\ln x\right]_B^{\infty}$$

Since W becomes infinite at the upper limit, assume F → 0 as x → 1000 B.

Then:

$$W = K \left[\ln x\right]_B^{1000B}$$

$$= K (\ln 1000 + \ln B - \ln B)$$

$$= K \ln 1000$$

$$= 6.9 K$$

n = 2

$$W = K \int_B^\infty \frac{dx}{x^n}$$

$$= K \int_B^\infty \frac{dx}{x^2}$$

$$= K \left[\frac{1}{x} \right]_B^\infty$$

$$= \frac{K}{B}$$

n = 3

$$W = \int_B^\infty \frac{dx}{x^n}$$

$$= K \int_B^\infty \frac{dx}{x^3}$$

$$= -K \left[\frac{1}{2x^2} \right]_B^\infty$$

$$= \frac{K}{2B^2}$$

n = 4

$$W = K \int_B^\infty \frac{dx}{x^n}$$

$$= K \int \frac{dx}{x^4}$$

$$= -K \left[\frac{1}{3x^3} \right]_B^\infty$$

$$= \frac{K}{3B^3}$$

Other Bonding

n = 1

$$W = \frac{K}{B^{n-1}} \int_{\theta_1}^{\pi/2} \cos^{n-2}$$

$$W = K \int_{\theta_1}^{\pi/2} \frac{\sin \theta}{\cos \theta} d\theta$$

$$= -K \left[\ln \cos \theta\right]_{\theta_1}^{\pi/2}$$

Since ln cos $\pi/2$ is $-\infty$ it will be necessary to assume that the upper limit is restricted to a value of θ such that $F \rightarrow 0$ as x or $\theta \rightarrow$ 1000B $< \theta = \pi/2$ then:

$$W = K (6.9 + \ln \cos \theta_1)$$

n = 2

$$W = \frac{K}{B^{n-1}} \int_{\theta_1}^{\pi/2} \cos^{n-2} \theta \sin \theta \, d\theta$$

$$= \frac{K}{B} \int_{\theta_1}^{\pi/2} \sin \theta \, d\theta$$

$$= -\frac{K}{B} \left[\cos \theta\right]_{\theta_1}^{\pi/2}$$

$$= \frac{K}{B} \cos \theta_1$$

n = 3

$$W = \frac{K}{2B^2} (\cos^2 \theta_1)$$

n = 4

$$W = \frac{K}{3B^3} (\cos^3 \theta_1)$$

Evaluation of W

If it can be assumed that the removed particles are hemispherical single crystal material, of radius R independent of crystal orientation and that a hemisphere of relatively large radius can be approximated by a stepped crystal lattice, then the pieces removed and the number of bonds broken in the process of removal can be computed. The following nomenclature for the broken bonds will be followed:

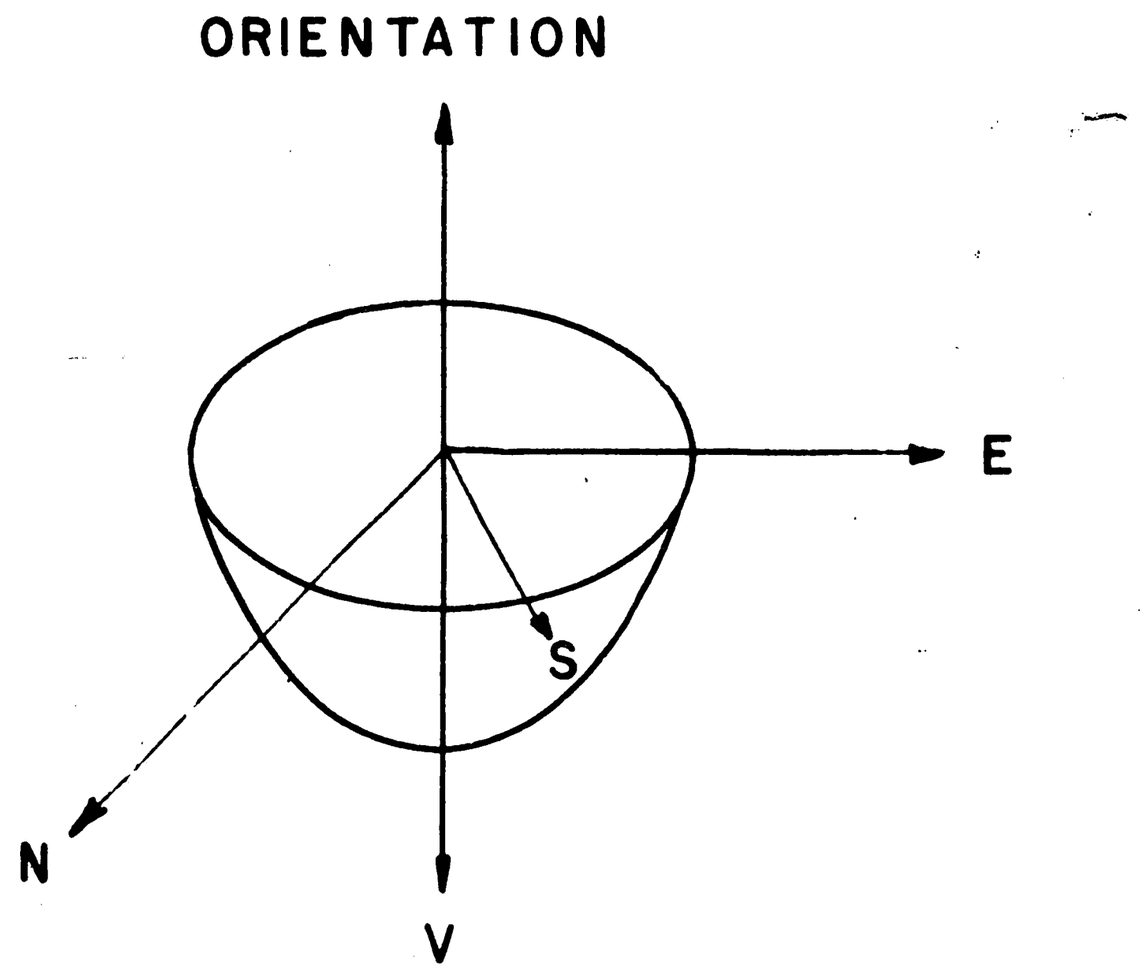

Orientation - The growth axis being machined

E and N - horizontal bonds (in the case of an[001]crystal E and N will have lattice parameter "a" and in[100] crystal E and N will have lattice parameters of "a" and "c" respectively.

V - vertical bonds

S - skewed or other than vertical or horizontal bonds.

In the horizontal directions, the projected area of hemisphere is $\frac{\pi R^2}{2}$ and in the vertical direction the area is πR^2.

The number of bonds broken in removing a hemisphere of material is equal to the product of the number of atoms per unit cell, the projected area of the hemisphere per cell area, the number of projected area faces, and the number of bonds per atom.

For an[001]crystal, the number of horizontal, bonds, N_N and N_E, vertical bonds N_V and skewed bonds N_S are

$$N_E = 2 \times \frac{\pi R^2}{2} \times \frac{1}{ac} \times 2 \times 1 = \frac{2\pi R^2}{ac}$$

$$N_N = 2 \times \frac{\pi R^2}{2} \times \frac{1}{a^2} \times 2 \times 1 = \frac{2\pi R^2}{ac}$$

$$N_V = 2 \times \pi R^2 \times \frac{1}{a^2} \times 1 \times 1 = \frac{2\pi R^2}{a^2}$$

$$N_S = 2 \times \frac{\pi R^2}{2} \times \frac{1}{ac} \times 2 \times 2 = \frac{4\pi R^2}{ac}$$

Similarly, for a[100]crystal:

$$N_E = \frac{2\pi R^2}{a^2}$$

$$N_N = \frac{2\pi R^2}{ac}$$

$$N_V = \frac{2\pi R^2}{ac}$$

$$N_s = \frac{4\pi R^2}{a^2}$$

The energy, or work, W, required to break these bonds is

$$W = \text{number of bonds x energy/bond.}$$

For any crystal

$W_{total} = W_N + W_E + W_V + W_S$, the sum of the energies required to break N, E, V and S bonds.

For an [001] crystal and the exponent n = 1

$$W^1_{001} = 6.9K \frac{2\pi R^2}{ac} + 6.9K \frac{2\pi R^2}{ac} + 6.9K \frac{2\pi R^2}{a^2} + (6.9 + \ln \cos 21.1)K \frac{4\pi R^2}{ac}$$

For Beta tin a = 5.818 and c = 3.174. Substituting

$$W^1_{001} = .2350\ (6.9K\ 2\pi R^2)$$

For [100] crystal and n = 1

$$W^1_{100} = 6.9K \frac{2\pi R^2}{ac} + 6.9K \frac{2\pi R^2}{a^2} + 6.9K \frac{2\pi R^2}{ac} + (6.9 + \ln \cos 68.9^o)\ K \frac{4\pi R^2}{a^2}$$

Again, substituting a = 5.818 and c = 3.174

$$W^1_{100} = .1883\ (6.9K\ 2\pi R^2)$$

Similarly for n = 2, 3, and 4

$$W^2_{001} = .0524\ (2\pi R^2 K)$$

$$W^3_{001} = .00583\ (2\pi R^2 K)$$

$$W^4_{001} = .000908\ (2\pi R^2 K)$$

$$W^2_{100} = .0345\ (2\pi R^2 K)$$

$$W_{100}^{3} = .0034\ (2\pi R^2 K)$$

$$W_{100}^{4} = .000513\ (2\pi R^2 K)$$

Assuming the radius R and the proportionality constant K are independent of crystal orientation, the ratio of $\frac{W_{001}}{W_{100}}$ can be computed for n = 1, 2, 3, and 4.

n	W_{001}/W_{100}
1	1.25
2	1.52
3	1.70
4	1.77

Bibliography

1. A. L. Livshits, Electro-erosion Machining of Metals, London: Butterworths, 1960.

2. M. Barash, "Electric Spark Machining," International Journal of Machine Tool Design and Research, Vol. 2, No. 3, July 1962, p. 281-295.

3. Prof. Dr-Ing H. Opitz, "Metallurgical Aspects and Surface Characteristics," Metal Treatment and Drop Forging, Vol. 27, No. 177, June 1960, p. 237-250.

4. E. M. Williams, "Theory of Electric Spark Machining," Electrical-Engineering, Vol. 71, No. 3, March 1952, p. 257-260.

5. E. M. Williams and R. E. Smith, "Phenomena Accompanying Transient Low-Voltage Discharges in Liquid Dielectrics," AIEE Trans, Vol. 74, Part 1, May 1955, p. 167-169.

6. Margit Toth-Bitskey and Jeno Pocza, "Investigations into the Elementary Processes Occurring in Electro Spark Machining," Acta Physica, Vol. 12, Iss. 1, 1960, p. 77-83.

7. P. A. Farley, "Characteristics of Spark Erosion Circuits," Spark Machining Symposium, Birmingham, England, 1959.

8. B. D. Cullity, Elements of X-ray Diffraction, Reading, Mass., Addison-Wesley, 1956, p. 484.

9. C. S. Barrett, Structure of Metals, 2d Ed., McGraw-Hill, 1952, p. 537.

10. M. Cole and C. W. B. Grigson, "Technique for the Rapid Accurate and Strain Free Machining of Single Crystals," British Journal of Applied Physics, Vol. 12, Iss. 6, June 1961, p. 296-297.

11. Dieter Mueller and Heinz Wadewitz, "Observations on Electro-erosion of Monocrystals," Bergakademie, Vol. 14, No. 7, p. 524-528, July 1962, (Engineering Soc. Library translation)

12. B. Sestak and S. Libovicky, "The Formation of Dislocations by Spark Discharges," Engineers Digest, Vol. 21, Iss. 12, Dec. 1960, p. 169-170, 203.

13. B. Chalmers, Proc. Phys. Soc. (London), Vol. 7, 1935, p. 733.

Vita

The author spend his early years in Scotland where he obtained his pre-college education.

He obtained his B. S. in Mechanical Engineering at Purdue University, Lafayette, Indiana, in 1959 after which he was employed by the Western Electric Company.